Research article

Modulation of bone turnover aberration: A target for management of primary osteoporosis in experimental rat model

Enas A. Fouad-Elhady [a,*], Hadeer A. Aglan [b,c], Rasha E. Hassan [a], Hanaa H. Ahmed [b,c], Gilane M. Sabry [a]

[a] Biochemistry Department, Faculty of Science, Ain Shams University, Cairo, Egypt
[b] Hormones Department, Medical Research Division, National Research Centre, Giza, Egypt
[c] Stem Cells Lab, Center of Excellence for Advanced Sciences, National Research Centre, Giza, Egypt

ARTICLE INFO

ABSTRACT

Osteoporosis is a skeletal degenerative disease characterised by abnormal bone turnover with scant bone formation and overabundant bone resorption. The present approach was intended to address the potency of nano-hydroxyapatite (nHA), chitosan/hydroxyapatite nanocomposites (nCh/HA) and silver/hydroxyapatite nanoparticles (nAg/HA) to modulate bone turnover deviation in primary osteoporosis induced in the experimental model. Characterisation techniques such as TEM, zeta-potential, FT-IR and XRD were used to assess the morphology, the physical as well as the chemical features of the prepared nanostructures. The *in vivo* experiment was conducted on forty-eight adult female rats, randomised into 6 groups (8 rats/group), (1) gonad-intact, (2) osteoporotic group, (3) osteoporotic + nHA, (4) osteoporotic + nCh/HA, (5) osteoporotic + nAg/HA and (6) osteoporotic + alendronate (ALN). After three months of treatment, serum sclerostin (SOST), bone alkaline phosphatase (BALP) and bone sialoprotein (BSP) levels were quantified using ELISA. Femur bone receptor activator of nuclear factor-kappa B (NF-κB) ligand (RANKL) and cathepsin K (CtsK) mRNA levels were evaluated by quantitative RT-PCR. Moreover, alizarin red S staining was applied to determine the mineralisation intensity of femur bone. Findings in the present study indicated that treatment with nHA, nCh/HA or nAg/HA leads to significant repression of serum SOST, BALP and BSP levels parallel to a significant down-regulation of RANKL and CtsK gene expression levels. On the other side, significant enhancement in the calcification intensity of femur bone has been noticed. The outcomes of this experimental setting ascertained the potentiality of nHA, nCh/HA and nAg/HA as promising nanomaterials in attenuating the excessive bone turnover in the primary osteoporotic rat model. The mechanisms behind the efficacy of the investigated nanostructures involved the obstacle of serum and tissue indices of bone resorption besides the strengthening of bone mineralisation.

1. Introduction

Osteoporosis is a chronic bone lytic disorder with a multifactorial aetiology and complicated pathophysiology [1]. The main reason is the imbalance in bone remodelling; between the two integrated processes, osteoblastic bone formation and osteoclastic bone resorption [2]. Estrogen plays a crucial role in the preservation of bone homeostasis [3]. Post-menopausal women, who are suffering from estrogen depletion, have more predisposition to develop osteoporotic fractures as a consequence of the accelerated bone turnover in line with increased number and activity of osteoclasts [1, 4]. Therefore, suppression of osteoclastogenesis is a propitious modality for treating pathological bone loss in osteoporotic subjects [5]. Current antiresorptive therapies comprise selective estrogen receptor modulators [6], bisphosphonates [7], denosumab [8], and strontium [9]. Despite these drugs show the desirable therapeutic effectiveness, the semipermanent use of them will bring about many adverse events in the long run, like gastrointestinal problems, typical femoral subtrochanteric fractures, and some drug-specific infections [10, 11]. In addition, estrogen replacement therapy is inadvisable as its risks exceed its benefits in older women [12]. Therefore, there is an unmet need for generating more specific new agents with less adverse effects.

Recently, much interest has emerged in the employment of nanomaterials as anti-osteoporosis candidates. In the setting of bone tissue

---

* Corresponding author.
  E-mail addresses: Enasfouad_p@sci.asu.edu.eg, ens_fd@yahoo.com (E.A. Fouad-Elhady).

engineering, there is a demand to create a biomaterial that mimics the native bone extracellular matrix. Natural bone consists of inorganic crystals (hydroxyapatite) and organic matrix (mainly type I collagen) [13].

Hydroxyapatite has been broadly applied as a biocompatible ceramic in several fields of medicine, particularly as bone substitutes, due to its similarity to the bone mineral. Owing to the nanostructure of bone tissue, nanonization of hydroxyapatite-based biocomposites is considered as the most promising challenge in bioceramics [14].

Chitosan-based hydroxyapatite biocomposite has been applied as scaffolding biomaterial in bone tissue engineering; chitosan/hydroxyapatite scaffolds offer competitive biocompatibility, osteoconductivity and biodegradability as well as remarkable mechanical properties for orthopaedic use [15].

Silver nanoparticles have been widely developed and characterised; they have shown good biocompatibility and antibacterial properties as well as *in vitro* osteoinductive potential [16]. Antibacterial susceptibility measurement, by the disc diffusion susceptibility test, proved that hydroxyapatite modified with nanosilver could be employed as an efficient antibacterial agent for orthopaedic implants [17]. Silver nanoparticles are the most recommended metal nanoparticles for formulating drug nano-carriers systems that have the ability to transport certain agents across the cell membrane [18].

This study was constructed to deliver proofs of concept for applicability and feasibility of nanotechnology in the intervention of osteoporosis *via* investigating the beneficial role of nanohydroxyapatite (nHA), chitosan/hydroxyapatite nanocomposites (nCh/HA) and silver/hydroxyapatite nanoparticles (nAg/HA) in modulating estrogen-depletion-mediated excessive bone turnover in the ovariectomized rat model representing primary osteoporosis.

2. Materials and methods

2.1. Nanomaterials

Nanohydroxyapatite, chitosan/hydroxyapatite nanocomposites and silver/hydroxyapatite nanoparticles were purchased from Nanotech Egypt (NanoTech Egypt for Photo- Electronics, City of 6 October, Giza, Egypt). Nanohydroxyapatite (nHA) was prepared by the wet chemical method, as reported by **Paz et al** [19]. Chitosan nanoplatform was prepared by the ionotropic gelation process stated by **Calvo et al** [20]. Silver/hydroxyapatite nanoparticles (nAg/HA) were generated according to the method described by **Ciobanu et al** [21].

2.1.1. Characterisation of nanomaterials

The morphology of the tested nanostructures was examined using high-resolution transmission electron microscopy (H-TEM, JEOL JEM-2100) operated at an accelerating voltage of 200 kV. Zeta-potential and dynamic light scattering (DLS) analyses of the nanomaterials were performed using Zetasizer ver. 6.32, Nano Series (Nano-ZS, Malvern Instruments, UK) which demonstrated their surface charge and the hydrodynamic size. Characterised functional groups of the nanoplatforms were identified from the Fourier Transform Infrared (FT-IR) spectra obtained by JASCO FT-IR-6800 spectrophotometer. Each spectrum was collected in the wavenumber range 400–4000 cm^{-1} and represented the average of a total of 8 scans performed at a resolution of 1 cm^{-1} in the transmission mode. X-ray diffraction (XRD) was applied to identify crystalline phases in a Philips X'pert X-ray diffractometer. The XRD patterns were conducted at room temperature in the 2θ scanning range of 0–$80°$ with a scan rate of $2°$ min^{-1} using monochromatized CuKα radiation of wavelength $= 1.5406$ A$°$ at 40 kV and 30 mA. Crystallite sizes L were determined from the Scherer's equation [22]:

$$[L = k\lambda / \beta \cos\theta]$$

where:

L: the average crystallite size

β: the full width of the peak at half of the maximum intensity (FWHM); radians

$\lambda = 1.5406$ $°$A

θ: Bragg's angle

$K = 0.9$; Scherrer's constant.

Graphical analysis was performed with the help of OriginPro 2018 software (OriginLab Corporation).

2.2. Animals and Experimentation

2.2.1. Animals

Adult female albino Wistar rats with 130–150 g weight were obtained from the Animal Care Unit of the National Research Centre, Giza, Egypt, and housed in well-ventilated area at the animal holding facility of Hormones Department at temperature (25 ± 1 °C) and humidity (55%) in plastic cages with stainless steel wire meshed covers. The animals were permitted to access freely to get water and standardized laboratory diet food for rodent for two weeks to be adapted to the new surroundings prior to the initiation of the experiment.

This study received approval. Animals care, surgical procedures and treatments were performed after receiving approval (number: 17/068) from the Medical Research Ethics Committee of National Research Centre, Giza, Egypt, and complied with the recommendations of the proper care and use of laboratory animals.

2.2.2. Induction of primary osteoporosis

Primary osteoporosis was induced in rats by surgical operation to remove the ovaries; under general anaesthesia using diethyl ether, the rats were bilaterally ovariectomized (OVX) by dorsal approach. The operation was performed at Hormones Department, Medical Research Division, National Research Centre. Ovariectomized rat is a well-established experimental model for primary osteoporosis that constitutes the alterations noticed in humans with more advantage; the therapeutic influences are detectable only few months after intervention. The ovariectomized rats, along with the gonad-intact rats, were left for 12 weeks.

2.2.3. Experimental design

The present experimental setup included forty-eight adult female rats which were assigned into six groups with eight rats per group: Group (1) Gonad-intact rats, Group (2) Osteoporotic rats. Group (3) osteoporotic rats treated intravenously with nanohydroxyapatite (8 mg/kg B.wt.) that is equivalent to 1/20 of the LD$_{50}$ reported previously by **Aoki et al** [23], once monthly for three months. Group (4) osteoporotic rats treated intravenously with chitosan/hydroxyapatite nanocomposite (8 mg/kg B.wt.) that is equivalent to 1/10 of the LD$_{50}$ reported by **Zhang et al** [24], once monthly for three months. Group (5) osteoporotic rats treated intravenously with silver/hydroxyapatite nanoparticle (8 mg/kg B.wt.) [25], once monthly for three months. Group (6) osteoporotic rats treated intragastrically with alendronate (Fosamax®, Merck & Co. Inc., Whitehouse Station, N.J., USA) (1 mg/kg B.wt.) once per week for three months [26].

After the termination of the treatment period, diets were withheld from the experimental rats for 12 h and then blood specimens were collected using a retro-orbital puncture under diethyl ether anaesthesia. The blood specimens were centrifuged, and the sera were divided into aliquots and kept at -80 °C for biochemical determinations. After sacrificing the rats by cervical dislocation, the femur bones of the hindlimb were harvested promptly from each rat, and the muscle tissue was scraped with sterile ophthalmic scissors and forceps. Some bones were fixed in neutral formalin (10%) for alizarin red S staining, and others

Table 1. Primers for GAPDH, RANKL and CtsK.

Genes	Primers	References
GAPDH	F: 5′-GTGGACCTCATGGCCTACAT-3`	[27]
	R: 5′-TGTGAGGGAGATGCTCAGTG-3`	
RANKL	F: 5′-CATCGGGTTCCCATAAAGTC-3`	[28]
	R: 5′-CTG-AAGCAAATGTTGGCGTA-3`	
CtsK	F: 5′-GCAGCAGAATGGAGGCATTG-3`	[29]
	R: 5′-TTCAGGGCTTTCTCGTTCCC-3`	

were preserved in liquid nitrogen and then kept at -80 °C for molecular genetics analyses.

2.3. Biochemical determinations

Serum SOST, BALP and BSP levels were quantified using commercially available ELISA kits (Kono Biotech Co., Ltd, China, catalogue number: KN0995Ra, KN0818Ra and KN0993Ra) according to the manufacturer manuals enclosed in the assay kits.

2.4. Molecular analyses for RANKL and CtsK genes

Total RNA was extracted from femur bone using SV whole RNA isolation system (Promega, Madison, WI, USA) according to the manufacturer's instruction. Concentration and purity of RNA were determined using the Nanodrop 2000 (Thermo Fisher Scientific, Waltham, MA, USA). The extracted RNA was reverse transcribed into cDNA using High-Capacity cDNA Reverse Transcription kits (Applied Biosystems, USA), under the guidance of the manufacturer. Glyceraldehyde 3-phosphate dehydrogenase (GAPDH) was the internal control. Primer sequences for GAPDH, RANKL and CtsK are shown in Table 1. Real-time PCR and data analyses were done using ViiA7 PCR cycler (Applied Biosystems, USA). Cycling conditions: cDNA synthesis for 10 min at 50 °C; inactivation of reverse transcription for 5 min at 95 °C; PCR amplification for 45 cycles with 10 s at 95 °C and 30 s at 60 °C. Melt curve analysis: 1 min at 95 °C, 1 min at 55 °C and 80 cycles of 10 s at 55–95 °C. Relative expression of the studied genes (RANKL and CtsK) was calculated using the comparative threshold cycle method. All values were normalised to the reference gene (GAPDH).

2.5. Alizarin Red S staining

Fixation of the compact femur bone of rats in 10% neutral formalin for 72 h, followed by decalcification in 15% neutral EDTA buffer. The decalcified compact bones were defatted and dehydrated with xylene and graded ethanol (50%–100%), then they were embedded in molten paraffin bee wax. For the alizarin red S staining, sections of 4 μm thickness were prepared; then the dehydrated slides were stained with alizarin red S solution for 2 min, the slides were rapidly dipped into acetone and acetone xylene (50/50), each for 20 s, respectively [30]. The average intensities of alizarin red S staining were quantified using IrfanView 4.53 software (a graphics software viewer).

2.6. Statistics

In the current study, all data were expressed as Mean ± standard error (S.E) of the mean. Data were analyzed by one-way analysis of variance (ANOVA) using the Statistical Package for the Social Sciences (SPSS) program, version 22 followed by Tukey's multiple comparison post-hoc test to compare significance between groups. The difference at $P < 0.05$, was considered significant.

3. Results

3.1. Characterisation of nanomaterials

3.1.1. Transmission electron microscopy (TEM)

The morphology of nHA, nCh/HA and nAg/HA were investigated using Transmission Electron Microscopy; high resolution (H-TEM). TEM micrographs showed that the nanostructures possess a rod-like shape (Figure 1). It can be noticed that the pure nHA ((Figure 1,a) exhibits an average length of less than 100 nm and diameter 20 ± 10 nm. The TEM imaging of nCh/HA (Figure 1,b), shows crystals in a polymer matrix with an average size of about 50 nm in length and 20 ± 10 nm in width. The morphology of nAg/HA by TEM (Figure 1,c), shows a uniform rod-like nano-crystallite with the main size of less than 100 nm and diameter 20 ± 10 nm.

3.1.2. Zeta-potential and dynamic light scattering (DLS) measurements

Values of the zeta-potential and the hydrodynamic size for the nHA, nCh/HA and nAg/HA, represented in Figure (2) were (-11.7 *mv*, 1091 nm), (-24.3 *mv*, 328.3 nm) and (-8.56 *mv*, 796.7 nm) respectively.

3.1.3. Fourier Transform Infrared (FT-IR) spectra

FT-IR analyses for nHA, nCh/HA and nAg/HA are represented in Figure (3). As shown in Figure (3,a), nHA characteristic bands are identified; vibrational bands of phosphate groups (PO_4^{3-}) at 1009, 570 and 556 cm^{-1} and stretching of hydroxyl group (O–H) at 3100–3520 cm^{-1}. The area at 3400 cm^{-1} mirrors the water adsorbed onto the surface of nHA [31]. Characteristic bands of the hydrogen phosphate group (HPO_4^{2-}) at 881 cm^{-1} are in conformity with the study of **Doat *et al*** [32] and the absorption bands of carbonate ion (CO_3^{2-}) at 1395 cm^{-1} are in agreement with the study of **Swain *et al*** [33].

The FT-IR spectrum of nCh/HA is shown in Figure (3,b), the marked nHA characteristic bands have appeared obviously; vibrational bands of PO_4^{3-}. The band assigned to the stretching vibration of
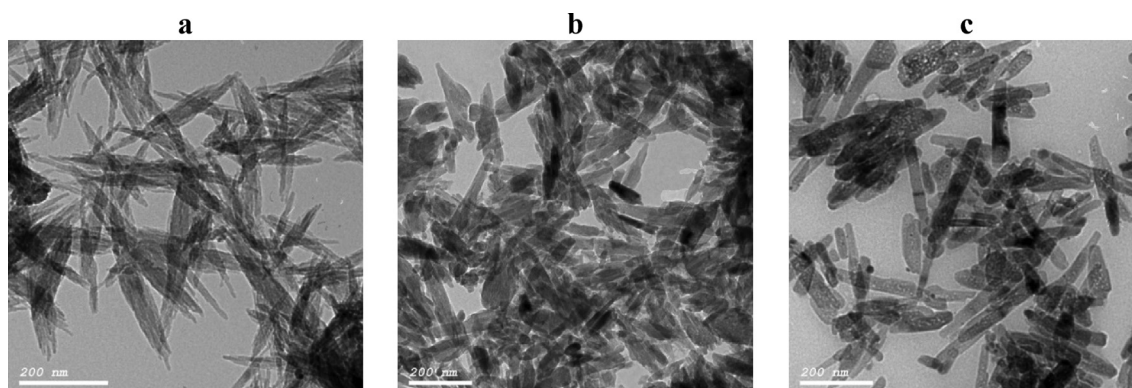

Figure 1. TEM micrographs of nHA (a), nCh/HA (b) and nAg/HA (c).

methylene group (-CH$_2$) at 2900 cm^{-1}, the stretching vibration of amide I (C=O) at 1627 cm^{-1}, the scissor vibration of amide II (N–H) at 1408 cm^{-1} and the stretching vibration of C–O at 1010 cm^{-1} documented the incorporation of chitosan in the nanocomposite (nCh/HA) [34].

Figure (3,c) shows the FT-IR spectrum of nanoAg-doped nHA structure. The FT-IR spectrum is similar to that of the undoped nHA, single-phase nanoparticles, except that more sharp band at 1635 cm^{-1} and wider broadband in region 3000 to 3600 cm^{-1} correspond to (H–O–H) bands of water lattice [35, 36] are observed in FT-IR spectrum of nAg/HA.

3.1.4. X-ray diffraction (XRD)

XRD is an analytical technique used to define and identify nano-materials and explain whether the sample materials are pure or contain impurities. X-ray diffraction pattern of nHA is depicted in Figure (4,a). The main diffraction peaks of nHA located at 2θ regions of 26°, 29°, 32°-34°, 40°, 46°-54° which are in coincidence with the data for standard hydroxyapatite phase of International Centre for Diffraction Data, Powder Diffraction File, standard card number 9-432 (ICDD-PDF No. 9-432) [37].

In Figure (4,b), X-ray diffraction pattern of nCh/HA, shows the appearance of the characteristic peaks of nHA, which match well with the
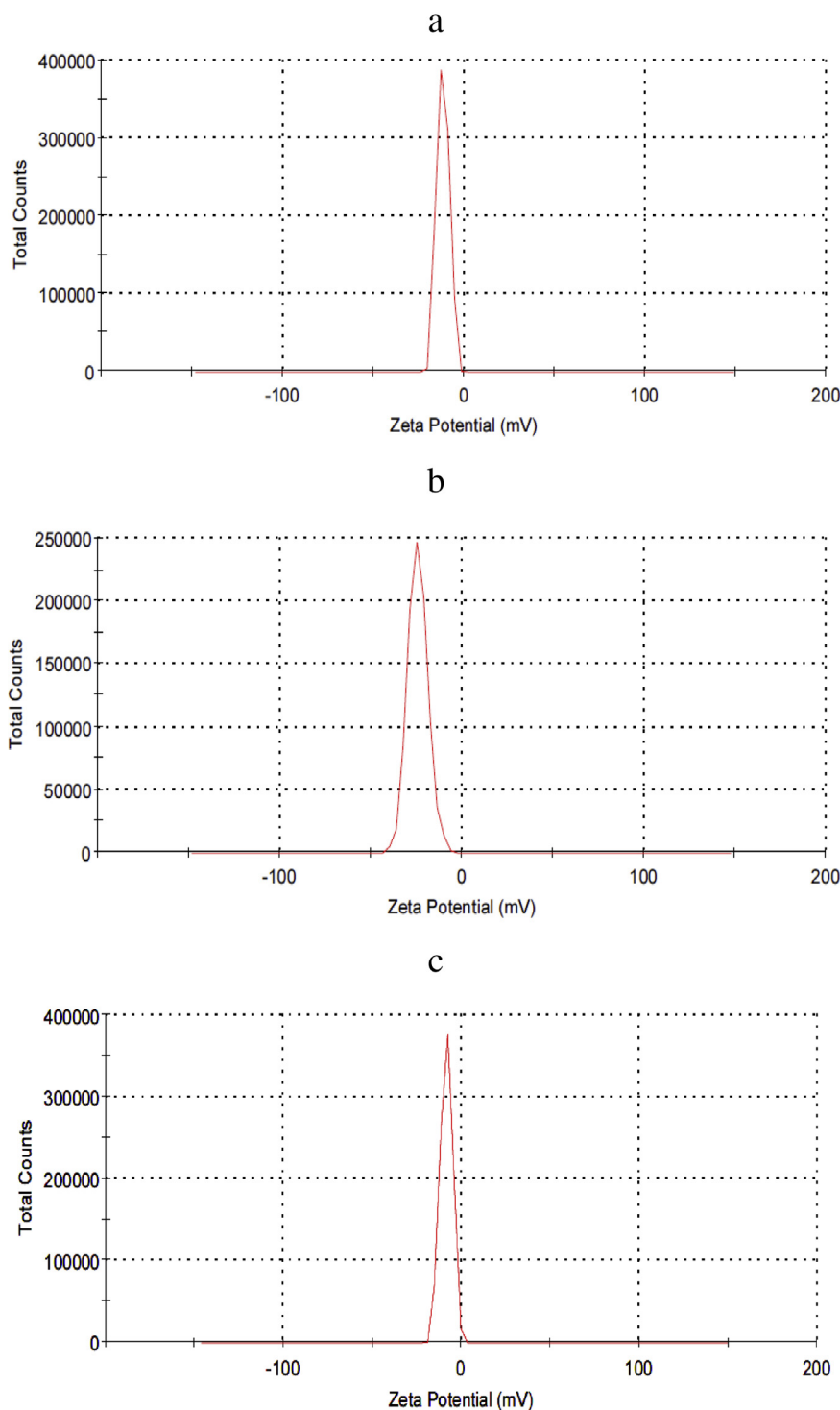
a

b

c

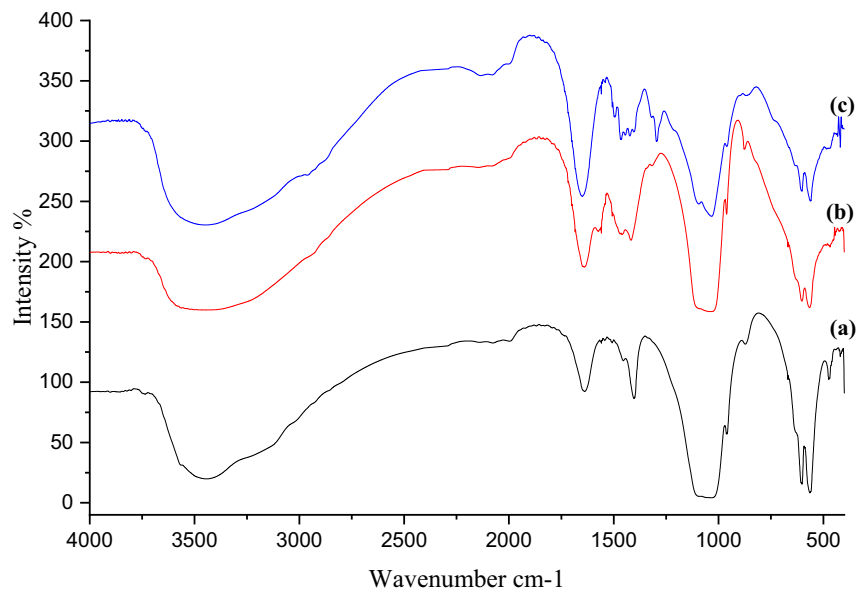**Figure 2.** Zeta potential for nHA (a), nCh/HA (b) and nAg/HA (c).

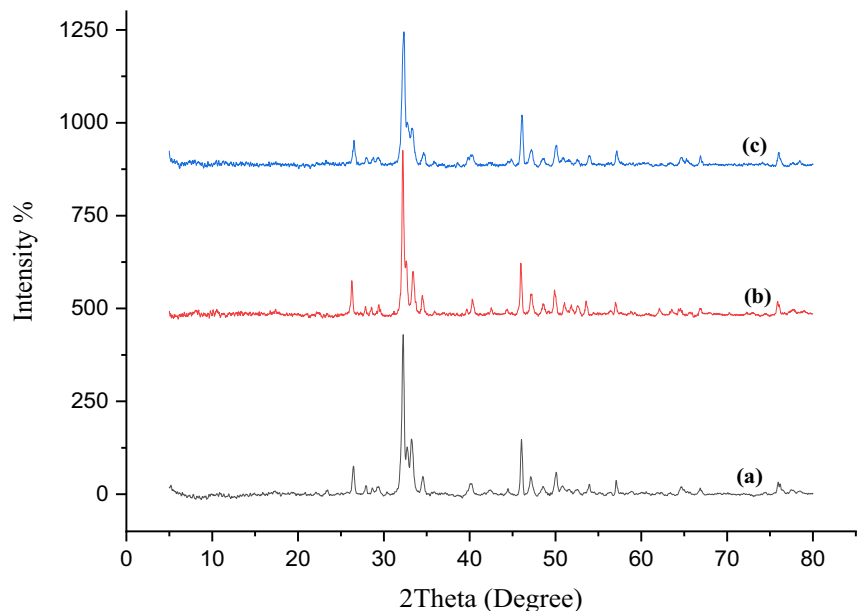**Figure 3.** FT-IR spectra for nHA (a), nCh/HA (b) and nAg/HA (c).

Figure 4. XRD diffractograms of nHA (a), nCh/HA (b) and nAg/HA (c).

data for standard hydroxyapatite phase, with the absence of the two main diffraction peaks of chitosan (at $2\theta = 10°$ and $20°$).

X-ray diffraction pattern of nAg/HA powder, illustrated in Figure (4,c), is similar to that of nHA; silver nanoparticle did not show specific diffraction pattern of silver nanoparticles.

The average crystallite sizes of nHA, nCh/HA, and nAg/HA were calculated by Scherrer's equation to affirm the nanoscale of the composites and was found to be 25.5, 28.85 and 22.73 nm, respectively.

3.2. Biochemical findings

The influence of nHA, nCh/HA and nAg/HA, as well as alendronate (ALN) on sera sclerostin (SOST) levels in osteoporotic rats, are given in Table 2. Serum SOST level elevated significantly ($P < 0.05$) by 48.74% in the osteoporotic group *versus* the gonad-intact group. Meanwhile, treatment with nHA, nCh/HA or nAg/HA produced a significant decrease ($P <$

0.05) in serum SOST level in comparison with the osteoporotic group. The per cent change in serum SOST level from the osteoporotic group was (-16.13%), (-15.69%) and (-13.43%) for nHA, nCh/HA and nAg/HA respectively. In osteoporotic rats received ALN, the decrease in serum SOST level was insignificant ($P > 0.05$), with per cent change of (-5.29%) relative to that of the osteoporotic group. Notably, serum SOST level showed a significant increase ($P < 0.05$) with per cent change of (40.86%) in the osteoporotic group treated with ALN *versus* the gonad-intact group. In comparison with ALN, the group administered nHA or nCh/HA showed a significant decrease ($P < 0.05$) in serum SOST level with per cent change of (-11.44%) and (-10.98%) respectively.

The alterations in serum bone alkaline phosphatase (BALP) level in the osteoporotic group following nHA, nCh/HA and nAg/HA as well as ALN treatment, are shown in Table 2. Serum BALP level elevated significantly ($P < 0.05$) by (48.07%) in the osteoporotic group when compared to the gonad-intact group. In contrast, it dropped significantly

Table 2. Effect of nHA, nCh/HA and nAg/HA as well as ALN on serum SOST, BALP and BSP levels in osteoporotic rats.

Groups	SOST (pg/mL)	BALP (ng/mL)	BSP (pg/mL)
Gonad-intact control	151.38 ± 4.57	23.313 ± 1.47	50.00 ± 2.49
Osteoporotic	225.15 ± 12.10*[a] (48.74%)	34.52 ± 1.35*[a] (48.10%)	87.51 ± 6.32*[a] (75.01%)
nHA	188.83 ± 2.26*[b] (-16.13%)	24.90 ± 1.68*[b] (-27.86%)	67.01 ± 3.94*[b] (-23.42%)
nCh/HA	189.81 ± 6.16*[b] (-15.69%)	25.97 ± 0.87*[b] (-24.76%)	68.06 ± 1.66*[b] (-22.22%)
nAg/HA	194.91 ± 3.00*[b] (-13.43%)	26.42 ± 0.78*[b] (-23.45%)	68.77 ± 2.97*[b] (-21.41%)
ALN	213.23 ± 7.12*[c*d] (-5.29%)	31.17 ± 1.93*[c*d*e] (-9.41%)	75.00 ± 2.00*[b] (-14.29%)

Data are expressed as Mean ± S.E for 8 rats/group.
*a: Significant change at P < 0.05 in comparison with the gonad-intact group.
*b: Significant change at P < 0.05 in comparison with the osteoporotic group.
*c: Significant change at P < 0.05 in comparison with the nHA-treated group.
*d: Significant change at P < 0.05 in comparison with the nCh/HA-treated group.
*e: Significant change at P < 0.05 in comparison with the nAg/HA-treated group.

(P < 0.05) in osteoporotic rats treated with either nHA, nCh/HA or nAg/HA by (-27.06%), (-24.76%) or (23.45%), respectively, compared to their osteoporotic counterparts. Serum BALP level repressed insignificantly (P > 0.05) in the osteoporotic group received ALN with per cent change of (-9.71%), as compared to the osteoporotic group. Moreover, the treatment of osteoporotic group with nHA, nCh/HA or nAg/HA revealed significant decline (P < 0.05) in serum BALP level, with per cent change of (-20.11%), (-16.84%) or (15.21%), respectively, in respect with osteoporotic group that received ALN. Noteworthy, the osteoporotic group treated with nHA showed that serum BALP level returned to near the normal value, where the per cent change from the gonad-intact group was only (6.81%).

The variations in serum bone sialoprotein (BSP) levels in the osteoporotic group treated with nHA, nCh/HA or nAg/HA, as well as ALN are represented in Table 2. Serum BSP level elevated significantly (P < 0.05) with per cent change of (75.01%) in the osteoporotic group *versus* the gonad-intact group. On the other side, serum BSP level was significantly blunted in all the treated groups in comparison with the osteoporotic group. Administration of nHA, nCh/HA, nAg/HA or ALN yielded significant reduction (P < 0.05) in serum BSP level relative to the osteoporotic group. The per cent change of serum BSP level from osteoporotic group was (-23.42%), (-22.22%), (-21.41%) and (-14.29%) for nHA, nCh/HA, nAg/HA and ALN, respectively.

3.3. Molecular outcomes

The influence of nHA, nCh/HA, nAg/HA and ALN treatments on nuclear factor-*kappa* B (NF-κB) ligand (RANKL) gene expression level in osteoporotic groups is illustrated in Table 3. The results demonstrated that RANKL gene expression level is significantly up-regulated (P < 0.05) in the osteoporotic group in comparison with the gonad-intact group

[fold change 1.81 *versus* 1.06, with a per cent change of (70.71%)]. On the opposite side, RANKL gene expression level was significantly down-regulated (P < 0.05) in all the treated groups *versus* the osteoporotic group. The per cent change of RANKL gene expression level from the osteoporotic group was (-50.23%), (-48.14%), (-34.89%) and (-26.67%) for nHA, nCh/HA, nAg/HA and ALN-treated groups, respectively.

Within the treated groups, administration of nHA or nCh/HA caused significant down-regulation (P < 0.05) in RANKL gene expression level in respect with those administered nAg/HA or ALN.

In comparison with the gonad-intact group, osteoporotic group treated with nHA or nCh/HA exhibited insignificant down-regulation (P > 0.05) in RANKL gene expression level with per cent change of (-15.31%) and (-11.75) for nHA and nCh/HA, respectively, while nAg/HA-treated group displayed insignificant up-regulation (P < 0.05) in RAKNL gene expression level with per cent change of (10.80%) from the gonad-intact group. Of note, the group that received ALN showed significant up-regulation (P < 0.05) in RANKL gene expression level with a per cent change of (24.70%) from the gonad-intact group.

The changes in cathepsin K (CtsK) gene expression level in osteoporotic groups following nHA, nCh/HA, nAg/HA or ALN treatments are depicted in Table 3. The results revealed that CtsK gene expression level is significantly up-regulated (P < 0.05) in the osteoporotic group in comparison with the gonad-intact group [fold change 1.88 *versus* 1.03, with a per cent change of (82.97%)]. All the treated groups exhibited significant down-regulation (P < 0.05) in CtsK gene expression level *versus* the osteoporotic group, as well as, the gonad-intact group with per cent change of (-70.73%), (-66.36%), (-64.20%) and (-62.47%) from the osteoporotic group, and (-46.44%), (-38.45%), (-34.50%) and (-31.33%) from the gonad-intact group for nHA, nCh/HA, nAg/HA and ALN-treated groups, respectively.

Table 3. Effect of nHA, nCh/HA and nAg/HA as well as ALN on RANKL and CtsK gene expression levels in osteoporotic rats.

Groups	Relative RANKL gene expression	Relative CtsK gene expression
Gonad-intact control	1.06 ± 0.15	1.03 ± 0.09
Osteoporotic	1.81 ± 0.066*[a] (70.16%)	1.88 ± 0.19*[a] (82.97%)
nHA	0.89 ± 0.039*[b] (-50.23%)	0.55 ± 0.054*[b] (-70.73%)
nCh/HA	0.94 ± 0.04*[b] (-48.14%)	0.63 ± 0.024*[b] (-66.36%)
nAg/HA	1.18 ± 0.038*[b*c*d] (-34.89%)	0.67 ± 0.022*[b] (-64.20%)
ALN	1.2 ± 0.053*[b*c*d] (-26.67%)	0.71 ± 0.035*[b] (-62.74%)

Data are expressed as Mean ± S.E for 8 rats/group.
*a: Significant change at P < 0.05 in comparison with the gonad-intact group.
*b: Significant change at P < 0.05 in comparison with the osteoporotic group.
*c: Significant change at P < 0.05 in comparison with the nHA-treated group.
*d: Significant change at P < 0.05 in comparison with the nCh/HA-treated group.
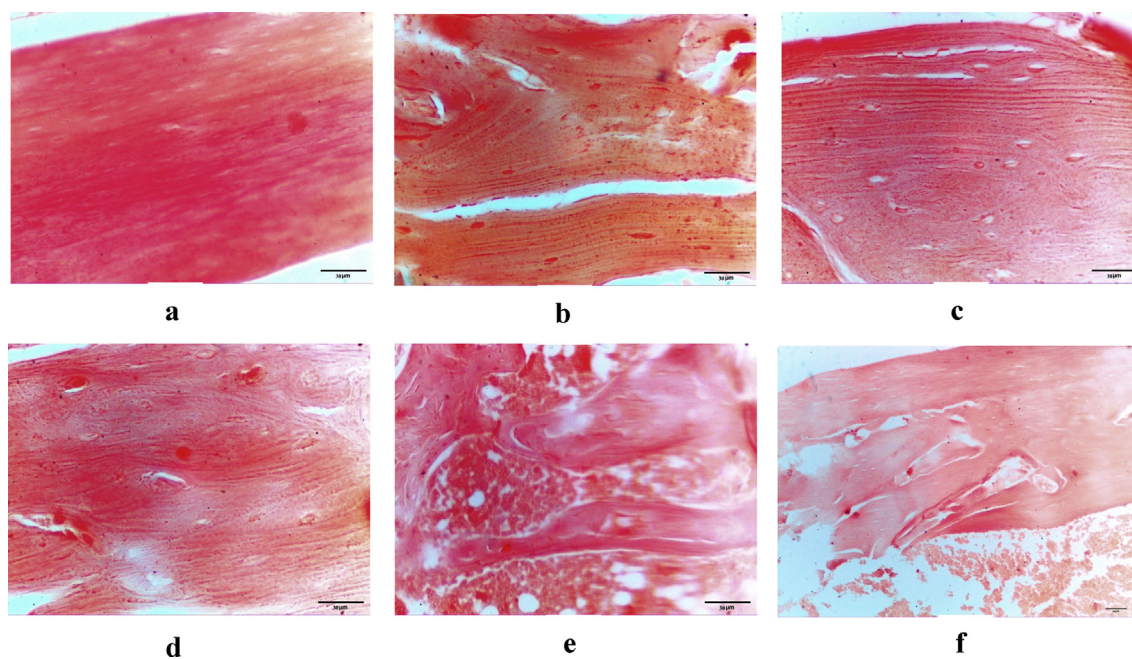
Figure 5. Longitudinal section of rat femur compact bone in; gonad-intact control rat (a), osteoporotic rat (b), nHA-treated rat (c), nCh/HA-treated rat (d), nAg/HA (e) and ALN-treated rat (f).

3.4. Mineralisation assay (Alizarin red S staining)

The optical micrographs of the longitudinal sections of femur compact bone from rats in the groups under study are represented in Figure (5, a-f). The degree of calcification (intensity of red colour) is markedly reduced in the bone of osteoporotic rats compared to that of gonad-intact rats [average 205.5 *versus* 251.97]. Among the treated groups, the maximum amount of alizarin red S staining (positive calcified bone) was noticed in nHA-treated group [235.41] followed by nCh/HA-treated group [234.62]. In nAg/HA-treated group, the amount of alizarin red S staining (positive calcified bone) [232.99] was lower than that in the previous two groups and followed by that of ALN-treated group [231.39].

4. Discussion

In the current research, TEM micrographs of nHA, nCh/HA and nAg/HA denoted that each prepared nanoplatforms is nano-sized with uniformity in shape. Zeta potential of the present study showed negative charge of the nanostructures in water dispersion. Numerous investigations on the zeta potential of synthetic bio-ceramics like hydroxyapatite and other calcium derivatives have exposed that a negative zeta potential improves the *in vivo* biological effects of the prepared micromaterials [38, 39]. It has been suggested that negative charges of the zeta potential have a valuable and promising outcome concerning the bone cell divisions and adhesions [39]. Negative zeta potential material is more convenient for osteoblasts adhesion and proliferation than neutral or positive material [38]. The presence of phosphate groups confers the negatively charged surface of the nanoparticles; however, positive calcium ions reduce this strong negative potential [31]. FT-IR has verified the presence of these groups. The existence of the positive and negative groups onto the surface of the nanoparticles represents their electrical features; which, in combination with their size, have a great impact on the biointegration characteristics [40]. Moreover, FT-IR spectra of nHA, nCh/HA and nAg/HA indicate the predominance of hydroxyapatite in both nCh/HA and nAg/HA composites.

Straight baseline and the sharp peaks of the XRD diffractogram of nHA proved that it is well crystallised and highly purified hydroxyapatite. In XRD diffractogram of nCh/HA, the appearance of the characteristic peaks of nHA, which match well with the data for standard hydroxyapatite phase, documented the occurrence of nHA crystallites after composite generation and revealed an interface binding between nHA and chitosan polymer matrix [41]. Absence of the characteristic peaks of chitosan points to the increase of nHA content in the composite [42]. Chitosan and nHA showed superb miscibility, there is no phase-separation. In the results of XRD for nAg/HA, there were no impurity phases (as Ag_3PO_4) denoting that Ag^+ enters the hydroxyapatite lattice by substituting Ca^{2+} [21]. So, the diffractogram of nAg/HA demonstrates its apatite characteristics with good crystallinity and purity.

The current *in vivo* study revealed that ovariectomy induces a significant increase in serum SOST level as compared to the gonad-intact counterparts. This finding matches that was observed by **Stegen *et al*** [43] and **Lin *et al*** [44] who indicated that, osteocytic SOST gene is overexpressed in ovariectomized mice with concomitant down-regulation of Wnt/β-catenin signalling leading to decreased bone mass. Interestingly, **Drake *et al*** [45] reported that peripheral SOST levels accurately reflect SOST levels in the bone microenvironment.

It has been reported that serum SOST level in postmenopausal women is markedly higher than that in premenopausal women [46]. In ovariectomized mice, SOST overexpression in bone cells by estrogen deficiency is reversed by estrogen replacement treatment [47]. Thus, administration of estrogen reduces, whilst deprivation of estrogen increases serum SOST levels. These findings obviously indicate that estrogen regulates circulating SOST levels and SOST expression in osteocytes [48]. The estrogenic signal is known to be transduced by two estrogen receptors, ER-α and ER-β [49]. ER-α could suppress SOST gene expression either genomically, direct binding to SOST gene promoter, or non-genomically via signalling pathways [50]. However, both ERα and ERβ mediate rapid activation of extracellular signal-regulated kinase (ERK) signalling in osteoblasts and osteocytes which inturn mediates SOST/sclerostin down-regulation by estrogen, so, inhibition of ERK activity due to estrogen depletion prevents SOST down-regulation [49]. Thus, estrogen and its receptor are essential for SOST expression down-regulation.

Estrogen deficiency stimulates T cells to produce the cytokine tumour necrosis factor-α (TNF-α) which mediates SOST overexpression through a proposed molecular mechanism where TNF-α up-regulates myocyte

enhancer factor 2 (MEF-2) [47]. It has been shown that MEF-2 is necessary to activate SOST expression in adult bones [51].

Intriguingly, **Zhao et al** [52] mentioned that the expression of hypoxia-inducible transcription factor-1α (HIF-1α) and pro-angiogenic factor Vascular endothelial growth factor (VEGF) decline owing to ovariectomy in female mice and that results in a reduction of bone volume and vasculature. Therefore, induction of HIF-1α signalling in bone cells preserves the skeletal vasculature and volume and could resist bone resorption observed in estrogen deficiency states. Normally, cortical osteocytes are surrounded by a hypoxic media [53] and these cells respond to hypoxia by prolyl hydroxylases (PHDs) axis which sense alterations of oxygen pressure and govern the HIF-1α abundance, the effector of the hypoxia response [43]. In hypoxia or anoxia, HIF-1α is translocated to the nucleus where it binds to HIF-1β then trigger the HIF-1 responsive genes which express the tissue adaptation to low oxygen tension [54]. Increased expression of osteoblastic HIF-1α down-regulates osteoclastic differentiation and activity to repress bone resorption [55]. Mechanistically, activated HIF-1α signalling elevates sirtuin1-dependent SOST promoter deacetylation, leading to suppression of SOST gene and, inconsequence, activation of Wnt/β-catenin signalling, on the other side, the sensation of oxygen by PHD2 in osteocytes up-regulates SOST epigenetically [43]. Therefore, estrogen deficiency increases PHD and decreases HIF-1α; ultimately resulting in SOST overexpression.

Treatment of osteoporotic rats with nanohydroxyapatite (nHA) brought about a significant reduction in serum SOST level in comparison with the untreated osteoporotic rats. Integrins on bone cell membrane interact with hydroxyapatite surfaces. These integrins recognize specific components of the extracellular matrix and mediate the stimulation and transduction of intracellular signals. Extracellular protein like focal adhesion kinase (FAK) is activated upon binding to integrin receptors, then a signal transduction proceeds. FAK association with Shc adaptor protein activates extracellular regulated kinases (ERK) signalling cascade via Ras [56], and hence, leads to transcription of various osteoblastic genes [57, 58]. Thus, ERK is activated in response to hydroxyapatite [59]. **Ha et al** [60] found that there is a fast and strong activation of the ERK1/2 pathway by nHA. As we mentioned above, the activation of ERK signalling in osteoblasts and osteocytes down-regulates SOST gene expression [49]. Therefore, the activation of ERK signalling module by nHA in the present study leads to the down-regulation of SOST gene expression.

A candidate factor involved in SOST down-regulation is prostaglandin E2 (PGE2), whose transcription is stimulated by cross-talk of ER and Wnt/β-catenin pathways. PGE2 enhances the expression of Wnt signalling responsive genes through suppression of SOST transcription in osteoblast [61]. It has been found that in osteoblast/osteoclast co-culture, micro-sized hydroxyapatite increases PGE2 concentrations 12.41 times over that of the control [62]. So nHA via promotion of ERK signalling axis and elevating the concentration of PGE2 could induce SOST/sclerostin down-regulation and thus decrease serum SOST level in osteoporotic rats.

Treatment of osteoporotic rats with nCh/HA produced a significant decrease in serum SOST level in comparison with the untreated osteoporotic rats. **Cui et al** [63] revealed that chitosan mediates corneal epithelial wound healing by augmenting ERK1/2 stimulation. Also, it has been commented that chitosan oligomers have suppressive effects of over-production of pro-inflammatory cytokine (TNF-α) in macrophage cells [64] and in murine RAW 264.7 cells [65]. As mentioned above, that activation of ERK signalling or suppression of TNF-α leads to down-regulation of SOST gene expression; therefore, nCh/HA could decrease serum SOST level via activation of ERK and inhibition of TNF-α production.

Treatment of osteoporotic rats with silver/hydroxyapatite nanoparticles caused a significant reduction in sera SOST levels when compared to the untreated osteoporotic rats. **Verano-Braga et al** [66], by performing a proteomic analysis, detected that extracellular exposure to nanosilver, 100 nm, can target intracellular responses via several

pathways including the mitogen-activated protein kinase (MAPK) pathway. MAPK/ERK is involved in the regulation of the osteoblast differentiation of skeletal stem cells [67]. Therefore, extracellular silver nanoparticles could stimulate bone formation [68]. **Kang et al** [69] found that SVEC4-10 cells (mouse endothelial cell line) treated with silver nanoparticles show increased activity of ERK1/2 compared to untreated cells. Thus, nAg/HA could produce SOST down-regulation via promotion of ERK signalling pathway.

MAPK pathway is implicated both in the regulation of HIF-1α protein formation [70] and potentiation of its transcriptional activity [71]. HIF-1α protein can be activated by direct phosphorylation by MAPK/ERK1/2 both in vitro and in vivo [72, 73]. Interestingly, **Cao et al** [68] and **Kang et al** [69] reported that silver nanoparticles activate MAPK/ERK. Silver nanoparticles could directly go into human MSCs, bind to DNA and stimulate the transcription of HIF-1α gene [74]. Additionally, in human lung carcinoma cells (A549), HIF-1α protein synthesis increased in states of hypoxia and in EC50 level (the effective concentration that causes 50% of the maximum effect) nanosilver treatment [75]. Similarly, nanosilver increases HIF-1α protein expression in hMSCs [74]. Gene expression analysis conducted on murine neural progenitor cells (C17.2) after treatment with non-toxic doses of silver nanoparticles showed up-regulation of various genes known to be targeted by HIF [76]. It is well known that HIF-1α supresses SOST gene expression [43].

It was proved that silver nanoparticles (10 nm) inhibit TNF-α gene expression [77]. Also, aqueous silver nanocrystals have an anti-inflammatory effect by lowering the pro-inflammatory mediators (TNF-α and histamine) level [78]. Moreover, silver nanoparticles have been found to suppress local inflammation in mouse mesenchymal stem cells (mMSCs) via reducing TNF-α level [79]. TNF-α is known to serve as a mediator for increased expression of SOST [47]. Therefore, nAg/HA could reduce serum SOST level in osteoporotic rats through stimulation of ERK1/2 pathway, activation of HIF-1α expression and also through the suppression of pro-inflammatory mediator (TNF-α) gene expression.

In the current study, ovariectomy induced significant elevation in serum bone alkaline phosphatase (BALP) level as compared to the gonad-intact group. This finding is in complete agreement with that of **Yu et al** [80] and **Khajuria et al** [81] who stated that serum level of BALP is significantly greater in the ovariectomized group than in the gonad-intact control group. Recently, **Yang et al** [82] indicated that ovariectomy elevates serum alkaline phosphatase (ALP) activity, and that reflects the greater degree of the ovariectomy-activated bone catabolism in comparison to the normal control. BALP is a glycoprotein osteoblast membrane-bound ectoenzyme; has extracellular catalytic subunit. Its primary function is to split the inorganic pyrophosphate (PPi) (a mineralisation inhibitor) and liberate inorganic phosphate [83]. BALP is produced by immature osteoblasts [84] and while its activity is essential for the induction of mineralisation, it is not involved in the resumption of this process [85] as early genes are turned off by a negative feedback loop [86]. Elevated bone turnover markers have been reported in the case of ovariectomy-induced decreased bone volume [87]. Ovariectomy or estrogen deficiency produces a significant increase in bone remodelling (turnover) in the two sides resorption and formation with more enhanced bone resorption resulting in bone loss [88]. **Lerner** [89] stated that in postmenopausal osteoporosis, the number of bone resorption sites and that of bone-formation sites are increased. Of note, BALP is liberated into the blood at the early stage of every bone-formation cycle [88] so the increase in its activity in the ovariectomized group is highly indicative of accelerated bone turnover.

Treatment of ovariectomized rats with nHA brought about significant drop in serum BALP level when compared to the untreated osteoporotic ones. This finding is in agreement with that of **Khajuria et al** [81], where the serum BALP level in the nanohydroxyapatite-administered group shows significant decline than that in the ovariectomized group. Furthermore, in vitro study of **Ha et al** [86] showed that nanohydroxyapatite induces a robust reduction of ALP and bone sialoprotein (BSP) mRNA levels in bone marrow mesenchymal stem cells (BMSCs)

and pre-osteoblasts, nanohydroxyapatite regulates *Alpl* (ALP gene) expression epigenetically through DNA methylation at its promoter region. In addition, various new genes were determined as nanohydroxyapatite target genes including insulin-like growth factor I and II (IGF-I and IGF-II) [60]. **Aeimlapa *et al*** [90] commented that IGF-I, which belongs to prominent cytokines for bone formation, is significantly increased in OVX rats. IGF-I induces alkaline phosphatase activity in primary rat calvaria cell culture, and IGF-II elevates alkaline phosphatase activity in human osteoblasts cultures [91, 92]. Moreover, at the cell surface, there are two specific hydroxyapatite sensors; phosphate-transporters (PiT) and fibroblast growth factor receptors (Fgfr) stimulating specific signalling proteins; Frs2α (Fgfr substrate 2α) and Erk1/2. In the case of BALP regulation, **Ha *et al*** [60] revealed that inhibition of Fgfr and PiT causes partial prohibition of repression of BALP gene expression and the stimulation of Fgfr and PiT by nanohydroxyapatite resulted in complete repression of BALP levels.

Treatment of osteoporotic rats with nCh/HA yielded significant depletion in serum BALP level when compared to the untreated osteoporotic rats. **Ma *et al*** [64] revealed that chitosan oligomers suppress the overshooting of the pro-inflammatory mediator (TNF-α) in the macrophage cells. Inhibition of TNF-α expression decreases serum BALP level [80]. It has been found that chitosan/metal composites enhance transcription of FGF-2 and TGF-β genes *in vitro* [93], FGF-2 could stimulate its receptor (Fgfr2) and repress BALP production. Furthermore, loss of estrogen represses the antioxidant processes within the bone, and this accounts for the elevated bone turnover due to the deprivation of this hormone [94]. In the study of **Jebahi *et al*** [95], the bioactive glass/-chitosan composite contributes to counteracting the oxidative process by favourably enhancing the antioxidant defence system. Consequently, chitosan could decrease bone turnover rate and in turn, reduce BALP serum level.

Treatment of osteoporotic rats with nAg/HA produced a significant decrease in serum BALP level when compared to the untreated osteoporotic rats. It has been reported that silver nanoparticles have anti-inflammatory effect *via* reduction of TNF-α [79]. **Yu *et al*** [80] found that TNF-α neutralising antibody treatment inhibits TNF-α expression and decreases serum BALP level as compared with OVX group. Hence, nAg/HA could decrease serum BALP level by inhibiting TNF-α expression. In addition, treatment of pregnant mice with nanosilver (8 nm) intravenously resulted in epigenetic methylation of several placental genes, among which, insulin-like growth factor 2 receptor (IGF-IIR) and IGF-II genes; indicating that exposure to nanosilver exerted significant suppression of IGF-IIR and IGF-II genes expression [96]. Overexpression of IGF-II has been detected to increase the alkaline phosphatase activity [92]. Thus, in the current study, the reduced serum BALP level could be attributed to the suppressive effect of nAg/HA on IGF-II gene expression.

Ovariectomy induced significant increase in serum bone sialoprotein (BSP) level as compared to the gonad-intact controls. This result comes in line with that obtained by **Shaarawy and Hasan** [97], where serum BSP is significantly increased in women after menopause compared to that of premenopausal ones. **Shaarawy and Hasan** [97] and **Singhal *et al*** [98] reported that aberrant elevated levels of serum BSP have been determined in numerous disorders characterised by hyperactivity of osteoclasts and increased bone resorption, involving osteoporosis and breast cancer with bone metastasis. Normally, continuous remodelling process of adult bone involves osteoclastic bone resorption and osteoblastic bone formation. Bone turnover regulator factors are produced by osteoclasts and osteoblasts. At the end of bone resorption and the beginning of bone formation, osteoblasts and osteocytes secrete matrix, called the reversal line, containing a plentiful amount of BSP and osteopontin (OPN) [99]. BSP mRNA reaches the highest concentration just preceding the mineralisation onset, and its protein is released by active osteoblasts that synthesise the matrix [100]. By a cell culture study, BSP has been detected to inhibit the formation of mature multinucleated osteoclasts from monocyte progenitors [101], even so, BSP and OPN promote mature osteoclasts to induce bone resorption [102]. From the

aforementioned data, it is reasonable to assume that the increase in BSP activity in the osteoporotic group in the current study reflects the excessive bone turnover due to estrogen deficiency.

Treatment of osteoporotic rats with nHA showed significant reduction in serum BSP concentration in comparison with the untreated osteoporotic rats. **Ha *et al*** [60] reported that BSP is down-regulated in BMSCs exposed to nanohydroxyapatite. Treatment of BMSCs or pre-osteoblasts with nanohydroxyapatite triggers an intensive dose-dependent inhibition of ALP and BSP genes expression. Nanohydroxyapatite generates a coordinated transcriptional regulation of BSP and ALP as a regulatory "program" which changes cell behaviour [86].

Treatment of osteoporotic rats with nCh/HA yielded a significant decline in serum BSP concentration when compared to the osteoporotic group. In clinical studies conducted on women, serum BSP levels are inversely correlated with that of estradiol [103]. Circulating BSP declined in response to therapies which resist bone resorption (hormone replacements) in line with a reduction in bone loss markers. Therefore, blood BSP could be a useful indicator for bone turnover [97]. **Chae *et al*** [104] indicated that there is an abnormal increase in count and surface of bone cells in ovariectomized rats as compared to sham-operated ones, and the supplementation of water-soluble chitosan inhibits this increase for seven weeks. Also, chitosan showed inhibitory effect on osteoclast resorption activity *in vitro* [105]. So, it could be suggested that nCh/HA has antiresorptive effect that could modulate the excessive bone turnover rate and consequently, diminish serum BSP level.

Osteoporotic rats treated with nAg/HA showed significant drop in serum BSP level when compared to the untreated osteoporotic rats. Cells cultured on nAg-HA/TiAlZr expressed very limited concentration of BSP mRNA as compared to those cultured on TiAlZr alone [106] suggesting the superior suppressing effect of the silver-doped hydroxyapatite nanoparticles on BSP expression. Excessive and prolonged ROS production due to estrogen deficiency suppresses osteoblastic activity and reduces bone formation [107]. Also, the increase in oxidative stress promotes the syntheses of pro-inflammatory molecules (IL-1, IL-6 and TNF-α) which trigger bone damage and enhance osteoclastic activity, thus disturbing the bone remodelling balance [108]. It has been reported that silver hydroxyapatite nanoparticles attenuate the inflammatory effect by decreasing the syntheses of the pro-inflammatory mediators like TNF-α and IL-1 [109]. **Nakayama *et al*** [110] found that TNF-α stimulated BSP mRNA expression at three hours of incubation with Saos2 osteoblast-like cells. Therefore, the decreased serum BSP level could be due to the anti-inflammatory actions by nAg/HA.

Ovariectomized rats in the present investigation experienced significant up-regulation in nuclear factor-kappa B (NF-κB) ligand (RANKL) gene expression level *versus* the gonad-intact controls. This result matches that of **Zhou *et a.*** [111], who revealed that RANKL mRNA level is significantly elevated in the ovariectomized rats. **Chen *et al*** [112] reported a significantly high RANKL/OPG (osteoprotegerin) mRNA ratio in the ovariectomized rats as compared to the sham-operated ones. OPG is the decoy receptor of RANKL, thus it inhibits bone resorption [113]. RANKL is one of the TNF family cytokines; it promotes monocyte progenitors to develop into mature osteoclasts. Specifically, the receptor RANK-RANKL binding induces TNF receptor-associated factor 6 (TRAF6) adaptor protein to activate inhibitor kappa B (IκB) kinase which then stimulates its ubiquitin-dependent proteasomal dissociation. Thereafter, NF-κB is liberated from the NF-κB/IκB complex and get into the nucleus where it regulates RANKL responsive genes [114]. Also, RANKL promotes transcription factor activator protein 1 (AP-1) through MAPK stimulation [115]. Both NF-κB and AP-1 up-regulate the expression of nuclear factor of activated T cells-c1 (NFATc1), which is crucial for terminal osteoclastic differentiation, and hence regulate particular osteoclastic genes such as TRAP and cathepsin K (Ctsk) [116]. **Bord *et al*** [117] found that, in cell cultures, estrogen has been shown to stimulate OPG expression and inhibit RANKL expression; estrogen activates colony formation potentiality of CD34+ cells to a megakaryocytic phenotype after that, mature megakaryocytes show estrogen-stimulated alterations

in bone cytokines such as OPG and RANKL. So, RANKL overexpression in osteoporotic rats could be due to estrogen deficiency.

OPG is a Wnt/β-catenin target gene [118]. Thus, suppression of Wnt/β-catenin signalling in mature osteoblasts and osteocytes suppresses OPG expression and subsequently, stimulates osteoclast differentiation [119]. On the contrary, active osteoblastic Wnt/β-catenin stimulates OPG expression and suppresses osteoclast differentiation and bone resorption [120]. Because SOST antagonises the Wnt/β-catenin signalling, it is expected that alterations in SOST expression could resist resorption by managing OPG [121]. Elevated SOST level increases RANKL expression, whereas decreases OPG expression [122]. In the current study, ovariectomy leads to increased serum SOST level indicating for inactivation of Wnt/β-catenin axis that is resulting in suppression of OPG and stimulation of RANKL genes expression; this represents the suggested explanation for the overexpression of RANKL gene in the osteoporotic rats in the present study.

Treatment of osteoporotic rats with nHA caused significant decrease in RANKL mRNA level when compared to the untreated osteoporotic rats. This result is supported by the previous *in vitro* study of **Macmillan** *et al* [123] who proved that bone cells cultured on nanocrystalline hydroxyapatite possess normalised molecular pathways; normal osteoclastic functions such as (expression of TRAP and RANK, resorption pits formation within the usual size) and also normal osteoblastic functions including expression of OPG and RANKL. It has been reported that stimulation of Wnt signalling in osteoblasts inhibits RANKL mRNA and protein syntheses [124], while, OPG expression is detected to be up-regulated by active Wnt signalling in multipotent mesenchymal cell line [120]. Wnt pathway is inhibited by SOST [121]. Results of the current study showed a decline in serum SOST level in nHA-treated group, which reflects a suppression of SOST gene expression. Therefore, nHA could down-regulate RANKL gene expression *via* stimulating Wnt signalling through inhibiting SOST transcription.

Treatment of osteoporotic rats with nCh/HA caused a significant down-regulation in RANKL gene expression level when compared to the untreated osteoporotic rats. This finding is comparable with that obtained by **Zhang** *et al* [125] who reported that in chitosan oligosaccharide-treated osteoarthritis-induced rats, RANKL secretion is inhibited while OPG is enhanced, RANKL/OPG mRNA ratio is significantly decreased, and RNAKL/RANK mRNA ratio is decreased. ROS raises the count of osteoclasts and induces resorption *in vitro* and *in vivo* by provoking RANKL and TNF-α expression *via* NF-κB [126, 127]. Chitosan has anti-inflammatory and antioxidant effect through down-regulating the pro-inflammatory cytokines [80] and up-regulating the antioxidative enzymes [95]. Therefore, suppression of RANKL gene expression by nCh/HA could be owing to chitosan anti-inflammatory and antioxidant properties. Moreover, the current data showed a decreased serum SOST level in nCh/HA-treated group, and as we mentioned above, the diminution of SOST expression activates Wnt signalling axis and consequently inhibits RANKL gene expression; this could be considered as another interpretation for the suppression of RANKL gene expression level upon treatment with nCh/HA.

Treatment of osteoporotic rats with nAg/HA resulted in a significant down-regulation in RANKL gene expression level when compared to the untreated osteoporotic rats. Molecular investigations with murine C17.2 neural progenitor cells cultured on non-toxic silver nanoparticles concentrations showed stimulation of several HIF target genes [76]. Among these genes, the OPG gene which regulates bone homeostasis [128]. **Shao** *et al* [55] found that expression of OPG is up-regulated while no change observed in RANKL expression in the presence of HIF-1α with high concentration; elevated HIF-1α level could stimulate OPG expression by direct binding to its promoter site and through this signalling pathway it could down-regulate the activity of osteoclasts and suppress osteoclastogenesis. This might lead to the down-regulation of RANKL gene expression, as shown in the present investigation. Furthermore, **Park** *et al* [129] revealed that TNFα induces up-regulation of RANKL gene expression. **Franková** *et al* [77] indicated that silver nanoparticles

decrease the expression of TNF-α in primary cell cultures. The blockage of TNF-α functions prevented ovariectomy-induced bone resorption similarly as estrogen [130]. This fact represents good support for our result in proving the efficacy of nAg/HA in down-regulating RANKL gene expression level and thus it could resist bone loss.

Ovariectomized rats in the present work experienced significant up-regulation in cathepsin K (CtsK) gene expression *versus* the gonad-intact controls. This finding is consistent with the study of **Pandiarajan** *et al* [131] where a higher CtsK mRNA expression and other osteoclastic markers are observed in the osteoporotic group, indicating an increased number of mature osteoclasts is strived to resorb bone. CtsK, a cysteine lysosomal protease, is extensively produced by mature active osteoclasts, and it has been suggested to posse a crucial role in the degradation of bone mineral and collagen matrices and thus bone resorption [132]. Excessive expression of CtsK gene accelerates bone turnover and decreases the bone volume [133]. Genes expression of CtsK and TRAP in osteoclasts is regulated by nuclear factor of activated T-cells (NFATc1) [134]. **Pandiarajan** *et al* [131] mentioned that NF-κB and NFATc1 activation is observed in the ovariectomized group and can be correlated to estrogen depletion-mediated oxidative stress. Moreover, RANKL and BSP activate that key osteoclastogenesis regulator (NFATc1) and increase mRNA expression of osteoclast differentiation markers (CtsK and TRAP) [135]. Furthermore, **Wijenayaka** *et al* [136] reported that SOST up-regulates the expression of CtsK in osteocytes *in vitro*. In the present study, the osteoporotic group showed significant increase in serum SOST level as well as increased expression of RANKL and BSP which explains the up-regulation of CtsK gene expression.

Treatment of osteoporotic rats with nHA induced significant down-regulation of CtsK gene expression when compared to the untreated osteoporotic rats. **Guo** *et al* [137] reported that nanohydroxyapatite down-regulates NF-κB signalling in rat glioma C6 cells and human glioma U87MG ATCC cells; it decreases NF-κB p65 protein expression and blocks NF-κB p65 nuclear translocation in C6 cells. Active NF-κB in the nucleus binds to DNA as a polypeptide dimer p50/p65, p65 subunit is the essential regulator of CtsK gene transcription [138]. RANKL could stimulate CtsK expression; moreover, agents that act as regulators of RANKL expression in osteoblasts, could regulate CtsK expression as well. IGF-I has been reported as a stimulator for RANKL, so it is also a stimulator for CtsK gene expression [139]. **Ha** *et al* [60] revealed that nanohydroxyapatite down-regulates IGF-I and IGF-II gene expression. Thus, nHA could down-regulate RANKL expression and consequently, suppresses CtsK expression. So that, nHA could suppress CtsK gene expression through down-regulation of NF-κB signalling and IGF-I gene expression.

Treatment of osteoporotic rats with nCh/HA brought about significant down-regulation in CtsK gene expression level when compared to the untreated osteoporotic ones. It has been reported that chitosan nanoparticles down-regulate mRNA expression levels of toll-like receptor 4 (TLR4) in LPS-inflamed Caco-2 cells [140]. TLR4 stimulates pro-inflammatory cytokines expression through the NF-κB signalling [141]. Oligochitosan significantly decreases NF-κB protein levels in LPS-induced RAW264.7 macrophages and consequently inhibits the excessive production of TNF-α and IL-1β [142]. Normally, NF-κB is kept attached to the inhibitory protein Iκ in the cytoplasm. Upon cell stimulation, IκB is phosphorylated and dissociated, p65 subunit of NF-κB will be released and inter the nucleus, binds to DNA and stimulates expression of NF-κB target genes [143] including CtsK gene [138]. Chitosan nanoparticles reduce dissotiation of IκB and prevent the translocation of p65 [140] which in turn suppress CtsK gene expression level as shown in the current results. Moreover, as chitosan/metal composites increase the expression of the anti-inflammatory cytokine (TGF-β) [93] and chitosan oligosaccharide inhibits RANKL while enhances OPG secretion [125], TGF-β inhibits CtsK gene expression through inhibiting RANKL expression while OPG directly suppresses CtsK gene expression [139].

Treatment of osteoporotic rats with nAg/HA yielded a significant down-regulation of CtsK gene expression level when compared to the

untreated osteoporotic rats. Biosynthesized silver nanoparticles have been shown to significantly diminish the concentrations of the inflammatory markers *via* NF-κB pathway [144] and the activated NF-κB stimulates expression of CtsK gene [138]. Silver nanoparticles (200 nm) can reduce DNA damage in diseased conditions that occurs *via* elevated TNF-α [145]. TNF-α is a mediator for increased expression of SOST [47], which in turn up-regulates the expression of CtsK in osteocytes *in vitro* [136]. So, the retraction of TNF-α by silver nanoparticles leads to the suppression of CtsK *via* inhibition of SOST.

Alizarin red S staining was applied for assessing the degree of mineralisation [146]. Alizarin red S staining interacts with calcium, that precipitates forming calcified nodules during the bone matrix deposition process [147]. Also, **Mathews *et al*** [148] mentioned that alizarin red S staining reacts with calcium inside cells and also calcium-binding proteins and proteoglycans.

In the current investigation, photomicrographs of femur bone from osteoporotic group showed an apparent depletion in the staining intensity as compared to the gonad-intact group. This observation comes in line with that of **Liu *et al*** [149] who revealed that the area of calcified nodules is obviously decreased in the femur bone of osteoporotic rats compared to that of gonad-intact control ones. Additionally, in the present investigation, the intensity of staining was greater in nHA-treated group as compared to the osteoporotic group. This is in agreement with *in vitro* study of **Dong *et al*** [150] who reported that treatment of BMSCs with nanohydroxyapatite leads to significant increase in bone mineralisation. Also, in the present study, the femur bone from osteoporotic rats treated with nCh/HA intensely stained with alizarin red S staining compared to osteoporotic counterparts. **Mathews *et al*** [148] indicated that chitosan enhances mineralisation by up-regulating genes accompanied with mineralisation and calcium-binding proteins. Finally, in the current work, the femur bone from osteoporotic rats administered nAg/HA showed a higher intensity of colour representing the alizarin red S staining in comparison with the osteoporotic rats. **Martínez-Sanmiguel *et al*** [109] stated that silver/hydroxyapatite nanoparticles have the ability to promote mineralisation/apatite nucleation *in vitro*.

In the present study, ALN was used as a reference drug to combat osteoporosis in the primary osteoporotic rat model. Treatment of osteoporotic rats with ALN showed insignificant drop in serum SOST and BALP levels, significant reduction in serum BSP level, significant down-regulation of RANKL and CtsK gene expression level in association with an increase in femur bone calcification, as shown in the photomicrograph of ARS staining, in comparison with the untreated osteoporotic counterparts.

ALN treatment does not significantly decrease the number of sclerostin-positive osteocytes in mechanical-unloaded rats [151]. Meanwhile, **Kim *et al*** [152] revealed that postmenopausal women, with a completed ablation of remnant estrogen, treated ALN shows a slight decrease in serum SOST level. Serum estradiol level has been found to be increased upon ALN treatment in ovariectomized rats [153]. Estradiol is known to down-regulate SOST expression [47]. Thus ALN could decrease serum SOST level *via* encouraging serum estradiol level.

In an earlier clinical investigation, **Parker *et al*** [154] studied ALN for the management of primary hyperparathyroid-related osteoporosis, and they found that in ALN -treated primary hyperparathyroid patients for 12 months, BALP is significantly lower than that measured at the baseline. Similarly, 12-month ALN treatment decreases serum BALP level in postmenopausal women; this effect could be attributed to the significant suppression of bone turnover by ALN [155].

Seibel *et al* [156] reported that treatment with bisphosphonates (the family includes ALN) intravenously produces rapid significant depletion in serum BSP level in patients with malignant bone disorders. Postmenopausal osteoporotic patients treated with ALN for 12 months showed significant drop in serum BSP level [97]. A major effect of bisphosphonate depends primarily on the inhibition of osteoclast functions [157] then induction of osteoclastic apoptosis, leading to the suppression of bone resorption and the reduction of bone remodelling [158].

Bisphosphonates could inhibit bone resorption by attaching to hydroxyapatite binding sites, so disrupting the osteoclast adhesion to the bone surface and preventing the production of protons which are needed for resorbing bones [159].

Silva *et al* [160] reported that RANKL and OPG mRNA levels in the periapical lesion in ovariectomized rats are not affected by ALN treatment. While, an *in vitro* study speculated that bisphosphonates change the RANKL/OPG ratio in osteoblasts, elevating OPG synthesis and reducing RANKL, thus suppressing bone loss [161]. Treatment with ALN induces a reduction in the bone-resorptive cytokines expression (IL-1β, IL-6 and TNF-α) in the ovariectomized rats [160] and also in murine RAW264.7 cells [162]. **Diercke *et al*** [163] indicated that IL-1β could induce RANKL transcription in primary human cementoblasts. So that, ALN may down-regulate RANKL gene expression level *via* the inhibition of the inflammatory cytokines.

Muñoz-Torres *et al* [164] revealed that in postmenopausal women, serum CtsK decreases gradually after ALN treatment. A recent investigation by **Yu *et al*** [165] suggested that PI3K signalling is preferentially served for transporting and production of CtsK. ALN has been shown to inhibit PI3K signalling module [166], which may represent the proposed mechanism by which ALN could down-regulate CtsK gene expression level.

Osteoporotic rats treated with ALN showed strong intensity of ARS *versus* that of osteoporotic rats. **Imai *et al*** [167] found that ARS staining of ALN-treated human mandibular fracture haematoma-derived cells (MHCs) tends to be superior compared to that observed in the control cells.

Collectively, in the present approach, the characterisation of the nanomaterials under investigation (nHA, nCh/HA and nAg/HA) confirmed their rod-shaped nanoscale morphology carrying negative surface charges and possessing fingerprint IR bands. The diffractogram peaks matched well the data for standard HA phase. All in all, the general characterisation of the selected nanomaterials indicates the absence of impurities and proves the incorporation of chitosan or silver within nCh/HA or nAg/HA composites with the predominance of nHA.

The documents of bone loss in the osteoporotic rats in the current experiment are indicated *via* a high serum SOST, BALP and BSP concentrations, overexpression of RANKL and CtsK mRNA, and low calcification level of femur bone of these rats as compared to those in the gonad-intact counterparts. In contrast, treatment of osteoporotic rats with nHA, nCh/HA or nAg/HA succeeded to protect against bone loss in the experimental model of primary osteoporosis *via* reducing serum SOST level and reducing bone turnover rate which is evidenced by the decline in serum BALP and BSP levels. Moreover, suppressing osteoclastogenesis was confirmed *via* down-regulation of RANKL and matrix-degrading enzyme (CtsK) gene expression levels. In consequent with these events, the calcification intensity of femur bone is strengthened in respect to osteoporotic rats.

In conclusion, the present investigation provides experimental evidence for the effectiveness of nHA, nCh/HA and nAg/HA as a lead antiresorptive nanobiomaterials for the intervention of primary osteoporosis. The superior impact of nHA could be ascribed to its nano-size and shape, which closely mimic those of HA crystals in the natural bone. As leading results, administration of nAg/HA revealed protection against accelerated bone turnover in osteoporotic rats, but, some modifications regarding the technique used for bonding Ag with HA are required to fine-tune the composition of silver-doped hydroxyapatite. Also, dose and treatment duration need further investigation to gain better therapeutic impact.

Declarations

Author contribution statement

Enas A. Fouad-ElHady: Performed the experiments; Analyzed and interpreted the data; Contributed reagents, materials, analysis tools or data; Wrote the paper.

Hadeer A. Aglan: Performed the experiments; Analyzed and interpreted the data; Contributed reagents, materials, analysis tools or data.

Rasha E. Hassan, Gilane M. Sabry: Analyzed and interpreted the data; Wrote the paper.

Hanaa H. Ahmed: Conceived and designed the experiments; Contributed reagents, materials, analysis tools or data; Wrote the paper.

Competing interest statement

The authors declare no conflict of interest.

Additional information

No additional information is available for this paper.

References

[1] Z. Li, G. Yuan, X. Lin, Q. Liu, J. Xu, Z. Lian, F. Song, J. Zheng, D. Xie, L. Chen, X. Wang, H. Feng, M. Zhou, G. Yao, Dehydrocostus lactone (DHC) suppresses estrogen deficiency-induced osteoporosis, Biochem. Pharmacol. 163 (2019) 279–289.

[2] B.-J. Kim, Y.-S. Lee, S.-Y. Lee, W.-Y. Baek, Y.J. Choi, S.A. Moon, S.H. Lee, J.-E. Kim, E.-J. Chang, E.-Y. Kim, J. Yoon, S.-W. Kim, S.H. Ryu, S.-K. Lee, J.A. Lorenzo, S.H. Ahn, H. Kim, K.-U. Lee, G.S. Kim, J.-M. Koh, Osteoclast-secreted SLIT3 coordinates bone resorption and formation, J. Clin. Invest. 128 (4) (2018) 1429–1441.

[3] J.A. Cauley, Estrogen and bone health in men and women, Steroids 99 (2015) 11–15.

[4] P. D'Amelio, A. Grimaldi, S. Di Bella, S.Z.M. Brianza, M.A. Cristofaro, C. Tamone, G. Giribaldi, D. Ulliers, G.P. Pescarmona, G. Isaia, Estrogen deficiency increases osteoclastogenesis up-regulating T cells activity: a key mechanism in osteoporosis, Bone 43 (1) (2008) 92–100.

[5] H. Jin, L. Yao, K. Chen, Y. Liu, Q. Wang, Z. Wang, Q. Liu, Z. Cao, J. Kenny, J. Tickner, X. Wang, J. Xu, Evodiamine inhibits RANKL-induced osteoclastogenesis and prevents ovariectomy-induced bone loss in mice, J. Cell Mol. Med. 23 (1) (2019) 522–534.

[6] B. Ettinger, D.M. Black, B.H. Mitlak, R.K. Knickerbocker, T. Nickelsen, H.K. Genant, C. Christiansen, P.D. Delmas, J.R. Zanchetta, J. Stakkestad, C.C. Gluer, K. Krueger, F.J. Cohen, S. Eckert, K.E. Ensrud, L.V. Avioli, P. Lips, S.R. Cummings, Reduction of vertebral fracture risk in postmenopausal women with osteoporosis treated with raloxifene: results from a 3-year randomized clinical trial, *Multiple Outcomes of Raloxifene Evaluation (MORE) investigators*, J. Am. Med. Assoc. 282 (7) (1999) 637–645.

[7] M.H. Murad, M.T. Drake, R.J. Mullan, K.F. Mauck, L.M. Stuart, M.A. Lane, N.O. Abu Elnour, P.J. Erwin, A. Hazem, M.A. Puhan, T. Li, V.M. Montori, Comparative effectiveness of drug treatments to prevent fragility fractures: a systematic review and network meta-analysis, J. Clin. Endocrinol. Metabol. 97 (6) (2012) 1871–1880.

[8] H.G. Bone, R.B. Wagman, M.L. Brandi, J.P. Brown, R. Chapurlat, S.R. Cummings, E. Czerwiński, A. Fahrleitner-Pammer, D.L. Kendler, K. Lippuner, J.-Y. Reginster, C. Roux, J. Malouf, M.N. Bradley, N.S. Daizadeh, A. Wang, P. Dakin, N. Pannacciulli, D.W. Dempster, S. Papapoulos, 10 years of denosumab treatment in postmenopausal women with osteoporosis: results from the phase 3 randomised FREEDOM trial and open-label extension, Lancet Diabetes Endocrinol. 5 (7) (2017) 513–523.

[9] P.J. Meunier, C. Roux, E. Seeman, S. Ortolani, J.E. Badurski, T.D. Spector, J. Cannata, A. Balogh, E.-M. Lemmel, S. Pors-Nielsen, R. Rizzoli, H.K. Genant, J.-Y. Reginster, The effects of strontium ranelate on the risk of vertebral fracture in women with postmenopausal osteoporosis, N. Engl. J. Med. 350 (5) (2004) 459–468.

[10] A. Qaseem, M.A. Forciea, R.M. McLean, T.D. Denberg, Treatment of low bone density or osteoporosis to prevent fractures in men and women: a clinical practice guideline update from the American college of physicians, Ann. Intern. Med. 166 (11) (2017) 818–839.

[11] V. Lagari, T. Gavcovich, S. Levis, The good and the bad about the 2017 American college of physicians osteoporosis guidelines, Clin. Therapeut. 40 (1) (2018) 168–176.

[12] M.K. Skjodt, M. Frost, B. Abrahamsen, Side effects of drugs for osteoporosis and metastatic bone disease, Br. J. Clin. Pharmacol. 85 (6) (2019) 1063–1071.

[13] M.R. Rogel, H. Qiu, G.A. Ameer, The role of nanocomposites in bone regeneration, J. Mater. Chem. 18 (36) (2008) 4233.

[14] S. Ribeiro, J. Costa-Rodrigues, M. Fernandes, Modulation of osteoclastogenesis by fluoroquinolones on nano- and micro-structured hydroxyapatite surfaces, Bone Abstracts 1 (2013) 220.

[15] L. Pighinelli, M. Kucharska, Chitosan–hydroxyapatite composites, Carbohydr. Polym. 93 (1) (2013) 256–262.

[16] Z. Mao, Y. Li, Y. Yang, Z. Fang, X. Chen, Y. Wang, J. Kang, X. Qu, W. Yuan, K. Dai, B. Yue, Osteoinductivity and antibacterial properties of strontium ranelate-loaded poly(lactic-co-glycolic acid) microspheres with assembled silver and hydroxyapatite nanoparticles, Front. Pharmacol. 9 (368) (2018) 1–13.

[17] R. Nirmala, F.A. Sheikh, M.A. Kanjwal, J.H. Lee, S.-J. Park, R. Navamathavan, H.Y. Kim, Synthesis and characterization of bovine femur bone hydroxyapatite containing silver nanoparticles for the biomedical applications, J. Nanoparticle Res. 13 (5) (2011) 1917–1927.

[18] P.K. Brown, A.T. Qureshi, A.N. Moll, D.J. Hayes, W.T. Monroe, Silver nanoscale antisense drug delivery system for photoactivated gene silencing, ACS Nano 7 (4) (2013) 2948–2959.

[19] A. Paz, D. Guadarrama, M. López, J.E. González, N. Brizuela, J. Aragón, A comparative study of hydroxyapatite nanoparticles synthesized by different routes, Quim. Nova 35 (9) (2012) 1724–1727.

[20] P. Calvo, C. Remunan-Lopez, J.L. Vila-Jato, M.J. Alonso, Novel hydrophilic chitosan-polyethylene oxide nanoparticles as protein carriers, J. Appl. Polym. Sci. 63 (1) (1997) 125–132.

[21] C. Ciobanu, S. Iconaru, P. Le Coustumer, L. Constantin, D. Predoi, Antibacterial activity of silver-doped hydroxyapatite nanoparticles against gram-positive and gram-negative bacteria, Nanoscale Res. Lett. 7 (1) (2012) 324.

[22] M. Shakir, R. Jolly, M.S. Khan, N. e Iram, H.M. Khan, Nano-hydroxyapatite/chitosan–starch nanocomposite as a novel bone construct: synthesis and in vitro studies, Int. J. Biol. Macromol. 80 (2015) 282–292.

[23] H. Aoki, H. Aoki, T. Kutsuno, W. Li, M. Niwa, An in vivo study on the reaction of hydroxyapatite-sol injected into blood, J. Mater. Sci. Mater. Med. 11 (2) (2000) 67–72.

[24] C. Zhang, G. Qu, Y. Sun, X. Wu, Z. Yao, Q. Guo, Pharmacokinetics, biodistribution, efficacy and safety of N-octyl-O-sulfate chitosan micelles loaded with paclitaxel, Biomaterials 29 (9) (2008) 1233–1241.

[25] N. Hadrup, K. Loeschner, A. Mortensen, A.K. Sharma, K. Qvortrup, E.H. Larsen, H.R. Lam, The similar neurotoxic effects of nanoparticulate and ionic silver in vivo and in vitro, Neurotoxicology 33 (3) (2012) 416–423.

[26] G.X. Chen, S. Zheng, S. Qin, Z.M. Zhong, X.H. Wu, Z.P. Huang, W. Li, R.T. Ding, H. Yu, J.T. Chen, Effect of low-magnitude whole-body vibration combined with alendronate in ovariectomized rats: a random controlled osteoporosis prevention study, PloS One 9 (5) (2014), e96181.

[27] K.Y. Chin, S. Abdul-Majeed, N. Mohamed, S. Ima-Nirwana, The effects of tocotrienol and lovastatin co-supplementation on bone dynamic histomorphometry and bone morphogenetic protein-2 expression in rats with estrogen deficiency, Nutrients 9 (2) (2017) 143.

[28] M. Cheng, T. Li, W. Li, Y. Chen, W. Xu, L. Xu, Leptin can promote mineralization and up-regulate RANKL mRNA expression in osteoblasts from adult female SD rats, Int. J. Clin. Exp. Pathol. 11 (3) (2018) 1610–1619.

[29] P. Govindarajan, W. Böcker, T. El Khassawna, M. Kampschulte, G. Schlewitz, B. Huerter, U. Sommer, L. Dürselen, A. Ignatius, N. Bauer, G. Szalay, S. Wenisch, K.S. Lips, R. Schnettler, A. Langheinrich, C. Heiss, Bone matrix, cellularity, and structural changes in a rat model with high-turnover osteoporosis induced by combined ovariectomy and a multiple-deficient diet, Am. J. Pathol. 184 (3) (2014) 765–777.

[30] Y. Guo, L. Wang, R. Ma, Q. Mu, N. Yu, Y. Zhang, Y. Tang, Y. Li, G. Jiang, D. Zhao, F. Mo, S. Gao, M. Yang, F. Kan, Q. Ma, M. Fu, D. Zhang, JiangTang XiaoKe granule attenuates cathepsin K expression and improves IGF-1 expression in the bone of high fat diet induced KK-Ay diabetic mice, Life Sci. 148 (2016) 24–30.

[31] L. Benedini, D. Placente, J. Ruso, P. Messina, Adsorption/desorption study of antibiotic and anti-inflammatory drugs onto bioactive hydroxyapatite nano-rods, Mater. Sci. Eng. C 99 (2019) 180–194.

[32] A. Doat, F. Pellé, N. Gardant, A. Lebugle, Synthesis of luminescent bioapatite nanoparticles for utilization as a biological probe, J. Solid State Chem. 177 (4–5) (2004) 1179–1187.

[33] S.K. Swain, S.V. Dorozhkin, Synthesis and dispersion of hydroxyapatite nanopowders, Mater. Sci. Eng. C 32 (5) (2012) 1237–1240.

[34] J. Zhang, C. Wang, J. Wang, Y. Qu, G. Liu, In vivo drug release and antibacterial properties of vancomycin loaded hydroxyapatite/chitosan composite, Drug Deliv. 19 (5) (2012) 264–269.

[35] D. Predoi, R.V. Ghita, M. Costache, D. Predoi, F. Ungureanu, C.C. Negrila, R.A. Vatasescu-Balcan, M. Costache, Characteristics of hydroxyapatite thin films, J. Optoelectron. Adv. Mater. 9 (12) (2007) 3827–3831.

[36] A. Costescu, I. Pasuk, F. Ungureanu, A. Dinischiotu, M. Costache, F. Huneau, S. Galaup, P. Coustumer, D. Le Predoi, Physico-chemical properties of nano-sized hexagonal hydroxyapatite powder synthesized by sol-gel, Digest J. Nanomater. Biostructures 5 (4) (2010) 989–1000.

[37] J.M. Chalovich, E. Eisenberg, The role of surface charge on the uptake and biocompatibility of hydroxyapatite nanoparticles with osteoblast cells, Nanotechnology 22 (10) (2011) 105708.

[38] N.C. Teng, S. Nakamura, Y. Takagi, Y. Yamashita, M. Ohgaki, K. Yamashita, A new approach to enhancement of bone formation by electrically polarized hydroxyapatite, J. Dent. Res. 80 (10) (2001) 1925–1929.

[39] J.J. Cooper, J.A. Hunt, The significance of zeta potential in osteogenesis, in: Annual Meeting Society for Biomaterials in Conjunction with the International Biomaterials Symposium, 29, 2006, p. 592 (2).

[40] H. Zhou, J. Lee, Nanoscale hydroxyapatite particles for bone tissue engineering, Acta Biomater. 7 (7) (2011) 2769–2781.

[41] M.R. Nikpour, S.M. Rabiee, M. Jahanshahi, Synthesis and characterization of hydroxyapatite/chitosan nanocomposite materials for medical engineering applications, Compos. Part B 43 (4) (2012) 1881–1886.

[42] Z. Li, L. Yubao, Y. Aiping, P. Xuelin, W. Xuejiang, Z. Xiang, Preparation and in vitro investigation of chitosan/nano-hydroxyapatite composite used as bone substitute materials, J. Mater. Sci. Mater. Med. 16 (3) (2005) 213–219.

[43] S. Stegen, I. Stockmans, K. Moermans, B. Thienpont, P.H. Maxwell, P. Carmeliet, G. Carmeliet, Osteocytic oxygen sensing controls bone mass through epigenetic regulation of sclerostin, Nat. Commun. 9 (1) (2018) 2557.

[44] C. Lin, X. Jiang, Z. Dai, X. Guo, T. Weng, J. Wang, Y. Li, G. Feng, X. Gao, L. He, Sclerostin mediates bone response to mechanical unloading through Antagonizing Wnt/β-catenin signaling, J. Bone Miner. Res. 24 (10) (2009) 1651–1661.

[45] M.T. Drake, B. Srinivasan, U.I. Mödder, J.M. Peterson, L.K. McCready, B.L. Riggs, D. Dwyer, M. Stolina, P. Kostenuik, S. Khosla, Effects of parathyroid hormone treatment on circulating sclerostin levels in postmenopausal women, J. Clin. Endocrinol. Metabol. 95 (11) (2010) 5056–5062.

[46] F.S. Mirza, I.D. Padhi, L.G. Raisz, J.A. Lorenzo, Serum sclerostin levels negatively correlate with parathyroid hormone levels and free estrogen index in postmenopausal women, J. Clin. Endocrinol. Metabol. 95 (4) (2010) 1991–1997.

[47] B.-J. Kim, S.J. Bae, S.-Y. Lee, Y.-S. Lee, J.-E. Baek, S.-Y. Park, S.H. Lee, J.-M. Koh, G.S. Kim, TNF-α mediates the stimulation of sclerostin expression in an estrogen-deficient condition, Biochem. Biophys. Res. Commun. 424 (1) (2012) 170–175.

[48] U. Il Mödder, J.A. Clowes, K. Hoey, J.M. Peterson, L. McCready, M.J. Oursler, B.L. Riggs, S. Khosla, Regulation of circulating sclerostin levels by sex steroids in women and in men, J. Bone Miner. Res. 26 (1) (2011) 27–34.

[49] G.L. Galea, L.B. Meakin, T. Sugiyama, N. Zebda, A. Sunters, H. Taipaleenmaki, G.S. Stein, A.J. Van Wijnen, L.E. Lanyon, J.S. Price, Estrogen receptor α mediates proliferation of osteoblastic cells stimulated by estrogen and mechanical strain, but their acute down-regulation of the Wnt antagonist Sost is mediated by estrogen receptor β, J. Biol. Chem. 288 (13) (2013) 9035–9048.

[50] R. Sapir-Koren, G. Livshits, Is interaction between age-dependent decline in mechanical stimulation and osteocyte-estrogen receptor levels the culprit for postmenopausal-impaired bone formation? Osteoporos. Int. 24 (6) (2013) 1771–1789.

[51] O. Leupin, I. Kramer, N.M. Collette, G.G. Loots, F. Natt, M. Kneissel, H. Keller, Control of the SOST bone enhancer by PTH using MEF2 transcription factors, J. Bone Miner. Res. 22 (12) (2007) 1957–1967.

[52] Q. Zhao, X. Shen, W. Zhang, G. Zhu, J. Qi, L. Deng, Mice with increased angiogenesis and osteogenesis due to conditional activation of HIF pathway in osteoblasts are protected from ovariectomy induced bone loss, Bone 50 (3) (2012) 763–770.

[53] J.A. Spencer, F. Ferraro, E. Roussakis, A. Klein, J. Wu, J.M. Runnels, W. Zaher, L.J. Mortensen, C. Alt, R. Turcotte, R. Yusuf, D. Côté, S.A. Vinogradov, D.T. Scadden, C.P. Lin, Direct measurement of local oxygen concentration in the bone marrow of live animals, Nature 508 (7495) (2014) 269–273.

[54] P.J. Ratcliffe, HIF-1 and HIF-2: working alone or together in hypoxia? J. Clin. Invest. 117 (4) (2007) 862–865.

[55] J. Shao, Y. Zhang, T. Yang, J. Qi, L. Zhang, L. Deng, HIF-1α disturbs osteoblasts and osteoclasts coupling in bone remodeling by up-regulating OPG expression, in: Vitro Cellular and Developmental Biology - Animal, 51, 2015, pp. 808–814 (8).

[56] S. Miyamoto, H. Teramoto, J.S. Gutkind, K.M. Yamada, Integrins can collaborate with growth factors for phosphorylation of receptor tyrosine kinases and MAP kinase activation: roles of integrin aggregation and occupancy of receptors, J. Cell Biol. 135 (6 Pt 1) (1996) 1633–1642.

[57] G. Xiao, R. Gopalakrishnan, D. Jiang, E. Reith, M.D. Benson, R.T. Franceschi, Bone morphogenetic proteins, extracellular matrix, and mitogen-activated protein kinase signaling pathways are required for osteoblast-specific gene expression and differentiation in MC3T3-E1 cells, J. Bone Miner. Res. 17 (1) (2002) 101–110.

[58] K. Mimori, M. Komaki, K. Iwasaki, I. Ishikawa, Extracellular signal-regulated kinase 1/2 Is involved in ascorbic acid–induced osteoblastic differentiation in periodontal ligament cells, J. Periodontol. 78 (2) (2007) 328–334.

[59] J.H. Song, J.H. Kim, S. Park, W. Kang, H.W. Kim, H.E. Kim, J.H. Jang, Signaling responses of osteoblast cells to hydroxyapatite: the activation of ERK and SOX9, J. Bone Miner. Metabol. 26 (2) (2008) 138–142.

[60] S.-W. Ha, J. Park, M.M. Habib, G.R. Beck, Nano-hydroxyapatite stimulation of gene expression requires Fgf receptor, phosphate transporter, and Erk1/2 signaling, ACS Appl. Mater. Interfaces 9 (45) (2017) 39185–39196.

[61] G. Zaman, A. Sunters, G.L. Galea, B. Javaheri, L.K. Saxon, A. Moustafa, V.J. Armstrong, J.S. Price, L.E. Lanyon, Loading-related regulation of transcription factor EGR2/Krox-20 in bone cells is ERK1/2 protein-mediated and prostaglandin, Wnt signaling pathway-, and insulin-like growth factor-I axis-dependent, J. Biol. Chem. 287 (6) (2012) 3946–3962.

[62] J.S. Sun, F.H. Lin, T.Y. Hung, Y.H. Tsang, W.H.S. Chang, H.C. Liu, The influence of hydroxyapatite particles on osteoclast cell activities, J. Biomed. Mater. Res. 45 (4) (1999) 311–321.

[63] R. Cui, Q. Lu, Y. Teng, K. Li, N. Li, Chitosan promoted the corneal epithelial wound healing via activation of ERK pathway, Curr. Eye Res. 42 (1) (2017) 21–27.

[64] P. Ma, H.T. Liu, P. Wei, Q.S. Xu, X.F. Bai, Y.G. Du, C. Yu, Chitosan oligosaccharides inhibit LPS-induced over-expression of IL-6 and TNF-α in RAW264.7 macrophage cells through blockade of mitogen-activated protein kinase (MAPK) and PI3K/Akt signaling pathways, Carbohydr. Polym. 84 (4) (2011) 1391–1398.

[65] H.J. Yoon, M.E. Moon, H.S. Park, S.Y. Im, Y.H. Kim, Chitosan oligosaccharide (COS) inhibits LPS-induced inflammatory effects in RAW 264.7 macrophage cells, Biochem. Biophys. Res. Commun. 358 (3) (2007) 954–959.

[66] T. Verano-Braga, R. Miethling-Graff, K. Wojdyla, A. Rogowska-Wrzesinska, J.R. Brewer, H. Erdmann, F. Kjeldsen, Insights into the cellular response triggered by silver nanoparticles using quantitative proteomics, ACS Nano 8 (3) (2014) 2161–2175.

[67] B.M. Abdallah, A. Jafari, W. Zaher, W. Qiu, M. Kassem, Skeletal (stromal) stem cells: an update on intracellular signaling pathways controlling osteoblast differentiation, Bone 70 (2015) 28–36.

[68] H. Cao, W. Zhang, F. Meng, J. Guo, D. Wang, S. Qian, X. Jiang, X. Liu, P.K. Chu, Osteogenesis catalyzed by titanium-supported silver nanoparticles, ACS Appl. Mater. Interfaces 9 (6) (2017) 5149–5157.

[69] K. Kang, D.H. Lim, I.H. Choi, T. Kang, K. Lee, E.Y. Moon, Y. Yang, M.S. Lee, J.S. Lim, Vascular tube formation and angiogenesis induced by polyvinylpyrrolidone-coated silver nanoparticles, Toxicol. Lett. 205 (3) (2011) 227–234.

[70] R. Fukuda, K. Hirota, F. Fan, Y. Do Jung, L.M. Ellis, G.L. Semenza, Insulin-like growth factor 1 induces hypoxia-inducible factor 1-mediated vascular endothelial growth factor expression, which is dependent on MAP kinase and phosphatidylinositol 3-kinase signaling in colon cancer cells, J. Biol. Chem. 277 (41) (2002) 38205–38211.

[71] J.I. Bárdos, M. Ashcroft, Hypoxia-inducible factor-1 and oncogenic signalling, Bioessays 26 (3) (2004) 262–269.

[72] D.E. Richard, E. Berra, E. Gothié, D. Roux, J. Pouysségur, p42/p44 mitogen-activated protein kinases phosphorylate hypoxia-inducible factor 1alpha (HIF-1alpha) and enhance the transcriptional activity of HIF-1, J. Biol. Chem. 274 (46) (1999) 32631–32637.

[73] A. Sodhi, S. Montaner, H. Miyazaki, J.S. Gutkind, MAPK and Akt act cooperatively but independently on hypoxia inducible factor-1α in rasV12 upregulation of VEGF, Biochem. Biophys. Res. Commun. 287 (1) (2001) 292–300.

[74] S.K. Jung, J.H. Kim, H.J. Kim, Y.H. Ji, J.H. Kim, S.W. Son, Silver nanoparticle-induced hMSC proliferation is associated with HIF-1-mediated upregulation of IL-8 expression, J. Invest. Dermatol. 134 (12) (2014) 3003–3007.

[75] J.-K. Jeong, S. Gurunathan, M.-H. Kang, J.W. Han, J. Das, Y.-J. Choi, D.-N. Kwon, S.-G. Cho, C. Park, H.G. Seo, H. Song, J.-H. Kim, Hypoxia-mediated autophagic flux inhibits silver nanoparticle-triggered apoptosis in human lung cancer cells, Sci. Rep. 6 (2016) 21688.

[76] B.B. Manshian, C. Pfeiffer, B. Pelaz, T. Heimerl, M. Gallego, M. Möller, P. del Pino, U. Himmelreich, W.J. Parak, S.J. Soenen, High-Content Imaging and Gene expression approaches to unravel the effect of surface functionality on cellular interactions of silver nanoparticles, ACS Nano 9 (10) (2015) 10431–10444.

[77] J. Franková, V. Pivodová, H. Vágnerová, J. Juránová, J. Ulrichová, Effects of silver nanoparticles on primary cell cultures of fibroblasts and keratinocytes in a wound-healing model, J. Appl. Biomater. Funct. Mater. 14 (2) (2016) 137–142.

[78] K. Chaloupka, Y. Malam, A.M. Seifalian, Nanosilver as a new generation of nanoproduct in biomedical applications, Trends Biotechnol. 28 (11) (2010) 580–588.

[79] R. Zhang, P. Lee, V.C.H. Lui, Y. Chen, X. Liu, C.N. Lok, M. To, K.W.K. Yeung, K.K.Y. Wong, Silver nanoparticles promote osteogenesis of mesenchymal stem cells and improve bone fracture healing in osteogenesis mechanism mouse model, Nanomed. Nanotechnol. Biol. Med. 11 (8) (2015) 1949–1959.

[80] Y. Yu, L. Lu, Z. Guo, Effect of TNF-α on osteoporosis by regulating the RANKL/OPG signaling pathway, Int. J. Clin. Exp. Med. 12 (6) (2019) 6925–6931.

[81] D.K. Khajuria, R. Razdan, D.R. Mahapatra, Development, in vitro and in vivo characterization of zoledronic acid functionalized hydroxyapatite nanoparticle based formulation for treatment of osteoporosis in animal model, Eur. J. Pharmaceut. Sci. 66 (2015) 173–183.

[82] H.J. Yang, M.J. Kim, J.Y. Qiu, T. Zhang, X. Wu, D. Jang, Rice porridge containing Welsh onion root water extract alleviates osteoarthritis-related pain behaviors, glucose levels, and bone metabolism in osteoarthritis-induced ovariectomized rats, Nutrients 11 (7) (2019) 1503.

[83] M.P. Whyte, Hypophosphatasia and the role of alkaline phosphatase in skeletal mineralization, Endocr. Rev. 15 (4) (1994) 439–461.

[84] Q. Wang, M. Alén, P.H.F. Nicholson, J.M. Halleen, S.L. Alatalo, C. Ohlsson, H. Suominen, S. Cheng, Differential effects of sex hormones on peri- and endocortical bone surfaces in pubertal girls, J. Clin. Endocrinol. Metabol. 91 (1) (2006) 277–282.

[85] N.M. Hooper, Glycosyl-phosphatidylinositol anchored membrane enzymes, Clin. Chim. Acta 266 (1) (1997) 3–12.

[86] S.-W. Ha, H.L. Jang, K.T. Nam, G.R. Beck, Nano-hydroxyapatite modulates osteoblast lineage commitment by stimulation of DNA methylation and regulation of gene expression, Biomaterials 65 (2015) 32–42.

[87] G. Girasole, N. Giuliani, A.B. Modena, G. Passeri, M. Pedrazzoni, Oestrogens prevent the increase of human serum soluble interleukin-6 receptor induced by ovariectomy in vivo and decrease its release in human osteoblastic cells in vitro, Clin. Endocrinol. 51 (6) (1999) 801–807.

[88] G.F. Zeng, Z.Y. Zhang, L. Lu, D.Q. Xiao, C.X. Xiong, Y.X. Zhao, S.H. Zong, Protective effects of Polygonatum sibiricum polysaccharide on ovariectomy-induced bone loss in rats, J. Ethnopharmacol. 136 (1) (2011) 224–229.

[89] U.H. Lerner, Bone remodeling in post-menopausal osteoporosis, J. Dent. Res. 85 (7) (2006) 584–595.

[90] R. Aeimlapa, K. Wongdee, W. Tiyasatkulkovit, K. Kengkoom, N. Krishnamra, N. Charoenphandhu, Anomalous bone changes in ovariectomized type 2 diabetic rats: inappropriately low bone turnover with bone loss in an estrogen-deficient condition, Am. J. Physiol. Endocrinol. Metabol. 317 (4) (2019) E646–E657.

[91] C. Schmid, T. Steiner, E.R. Froesch, Insulin-like growth factor I supports differentiation of cultured osteoblast-like cells, FEBS Lett. 173 (1) (1984) 48–52.

[92] D.D. Strong, A.L. Beachler, J.E. Wergedal, T.A. Linkhart, Insulinlike growth factor II and transforming growth factor β regulate collagen expression in human osteoblastlike cells in vitro, J. Bone Miner. Res. 6 (1) (1991) 15–23.

[93] Sivashankari, P. R., & Prabaharan, M., Bioactive Nanomaterials/chitosan Composites as Scaffolds for Tissue Regeneration. Polysaccharide Carriers for Drug Delivery. Woodhead Publishing.

[94] S.C. Manolagas, From estrogen-centric to aging and oxidative stress: a revised perspective of the pathogenesis of osteoporosis, Endocr. Rev. 31 (3) (2010) 266–300.

[95] S. Jebahi, H. Oudadesse, G. Ben Saleh, M. Saoudi, S. Mesadhi, T. Rebai, H. Keskes, A. el Feki, H. el Feki, Chitosan-based bioglass composite for bone tissue healing : oxidative stress status and antiosteoporotic performance in a ovariectomized rat model, Kor. J. Chem. Eng. 31 (9) (2014) 1616–1623.

[96] X.-F. Zhang, J.-H. Park, Y.-J. Choi, M.-H. Kang, S. Gurunathan, J.-H. Kim, Silver nanoparticles cause complications in pregnant mice, Int. J. Nanomed. 10 (2015) 7057–7071.

[97] M. Shaarawy, M. Hasan, Serum bone sialoprotein: a marker of bone resorption in postmenopausal osteoporosis, Scand. J. Clin. Lab. Investig. 61 (7) (2001) 513–522.

[98] H. Singhal, D.S. Bautista, K.S. Tonkin, F.P. O'Malley, A.B. Tuck, A.F. Chambers, J.F. Harris, Elevated plasma osteopontin in metastatic breast cancer associated with increased tumor burden and decreased survival, Clin. Canc. Res. Offic. J. Am. Assoc. Cancer Res. 3 (4) (1997) 605–611.

[99] K. Hultenby, F.P. Reinholt, Å. Oldberg, D. Heinegård, Ultrastructural immunolocalization of osteopontin in metaphyseal and cortical bone, Matrix 11 (3) (1991) 206–213.

[100] E.A. Cowles, M.E. DeRome, G. Pastizzo, L.L. Brailey, G.A. Gronowicz, Mineralization and the expression of matrix proteins during in vivo bone development, Calcif. Tissue Int. 62 (1) (1998) 74–82.

[101] B. Ganss, R.H. Kim, J. Sodek, Bone sialoprotein, Crit. Rev. Oral Biol. Med. 10 (1) (1999) 79–98.

[102] A.I. Alford, K.D. Hankenson, Matricellular proteins: extracellular modulators of bone development, remodeling, and regeneration, Bone 38 (6) (2006) 749–757.

[103] P. Pietschmann, S. Kudlacek, J. Grisar, S. Spitzauer, W. Woloszczuk, R. Willvonseder, M. Peterlik, Bone turnover markers and sex hormones in men with idiopathic osteoporosis, Eur. J. Clin. Invest. 31 (5) (2001) 444–451.

[104] H.J. Chae, G.Y. Lee, S.K. Yang, D.S. Kim, K.J. Yun, E.C. Kim, H.M. Kim, S.W. Chae, H.R. Kim, Effect of high molecular weight water-soluble chitosan on the trabecular bone and thickness in ovariectomized rats, Immunopharmacol. Immunotoxicol. 29 (3–4) (2007) 439–449.

[105] N. Rochet, T. Balaguer, F. Boukhechba, J.P. Laugier, D. Quincey, S. Goncalves, G.F. Carle, Differentiation and activity of human preosteoclasts on chitosan enriched calcium phosphate cement, Biomaterials 30 (26) (2009) 4260–4267.

[106] D. Ionita, M. Dilea, I. Titorencu, I. Demetrescu, Merit and demerit effects of silver nanoparticles in the bioperformance of an electrodeposited hydroxyapatite: nanosilver composite coating, J. Nanoparticle Res. 14 (10) (2012) 1152.

[107] V. Domazetovic, G. Marcucci, T. Iantomasi, M.L. Brandi, M.T. Vincenzini, Oxidative stress in bone remodeling: role of antioxidants, Clin. Cases Miner. Bone Metabol. 14 (2) (2017) 209–216.

[108] M. Capulli, R. Paone, N. Rucci, Osteoblast and osteocyte: games without frontiers, Arch. Biochem. Biophys. 561 (2014) 3–12.

[109] J.J. Martínez-Sanmiguel, D. G Zarate-Triviño, R. Hernandez-Delgadillo, A.L. Giraldo-Betancur, N. Pineda-Aguilar, S.A. Galindo-Rodríguez, M.A. Franco-Molina, S.P. Hernández-Martínez, C. Rodríguez-Padilla, Anti-inflammatory and antimicrobial activity of bioactive hydroxyapatite/silver nanocomposites, J. Biomater. Appl. 33 (10) (2019) 1314–1326.

[110] Y. Nakayama, N. Kato, Y. Nakajima, E. Shimizu, Y. Ogata, Effect of TNF-α on human osteosarcoma cell line Saos2 - TNF-α regulation of bone sialoprotein gene expression in Saos2 osteoblast-like cells, Cell Biol. Int. 28 (10) (2004) 653–660.

[111] J. Zhou, S. Chen, H. Guo, L. Xia, H. Liu, Y. Qin, C. He, Pulsed electromagnetic field stimulates osteoprotegerin and reduces RANKL expression in ovariectomized rats, Rheumatol. Int. 33 (5) (2013) 1135–1141.

[112] C. Chen, H. Zheng, S. Qi, Genistein and silicon synergistically protects against ovariectomy-induced bone loss through upregulating OPG/RANKL ratio, Biol. Trace Elem. Res. 188 (2) (2019) 441–450.

[113] B.F. Boyce, L. Xing, Functions of RANKL/RANK/OPG in bone modeling and remodeling, Arch. Biochem. Biophys. 473 (2) (2008) 139–146.

[114] D.V. Novack, Role of NF-κB in the skeleton, Cell Res. 21 (1) (2011) 169–182.

[115] J. Mizukami, G. Takaesu, H. Akatsuka, H. Sakurai, J. Ninomiya-Tsuji, K. Matsumoto, N. Sakurai, Receptor activator of NF-kB ligand (RANKL) activates TAK1 mitogen-activated protein kinase kinase kinase through a signaling complex containing RANK, TAB2, and TRAF6, Mol. Cell Biol. 22 (4) (2002) 992–1000.

[116] H. Takayanagi, S. Kim, T. Koga, H. Nishina, M. Isshiki, H. Yoshida, A. Saiura, M. Isobe, T. Yokochi, J. Inoue, E.F. Wagner, T.W. Mak, T. Kodama, T. Taniguchi, Induction and activation of the transcription factor NFATc1 (NFAT2) integrate RANKL signaling in terminal differentiation of osteoclasts, Dev. Cell 3 (6) (2002) 889–901.

[117] S. Bord, E. Frith, D.C. Ireland, M.A. Scott, J.I.O. Craig, J.E. Compston, Synthesis of osteoprotegerin and RANKL by megakaryocytes is modulated by oestrogen, Br. J. Haematol. 126 (2) (2004) 244–251.

[118] R. Baron, M. Kneissel, WNT signaling in bone homeostasis and disease: from human mutations to treatments, Nat. Med. 19 (2) (2013) 179–192.

[119] I. Kramer, C. Halleux, H. Keller, M. Pegurri, J.H. Gooi, P.B. Weber, J.Q. Feng, L.F. Bonewald, M. Kneissel, Osteocyte Wnt/β-catenin signaling is required for normal bone homeostasis, Mol. Cell Biol. 30 (12) (2010) 3071–3085.

[120] A. Jackson, B. Vayssière, T. Garcia, W. Newell, R. Baron, S. Roman-Roman, G. Rawadi, Gene array analysis of Wnt-regulated genes in C3H10T1/2 cells, Bone 36 (4) (2005) 585–598.

[121] M. Stolina, D. Dwyer, Q.-T. Niu, K.S. Villasenor, P. Kurimoto, M. Grisanti, C.-Y. Han, M. Liu, X. Li, M.S. Ominsky, H.Z. Ke, P.J. Kostenuik, Temporal changes in systemic and local expression of bone turnover markers during six months of sclerostin antibody administration to ovariectomized rats, Bone 67 (2014) 305–313.

[122] S.Y. Bai, Y. Chen, H.W. Dai, L. Huang, Effect of sclerostin on the functions and related mechanisms of cementoblasts under mechanical stress, West China J. Stomatol. 37 (2) (2019) 162–167.

[123] A.K. Macmillan, F.V. Lamberti, J.N. Moulton, B.M. Geilich, T.J. Webster, Similar healthy osteoclast and osteoblast activity on nanocrystalline hydroxyapatite and nanoparticles of tri-calcium phosphate compared to natural bone, Int. J. Nanomed. 9 (1) (2014) 5627–5637.

[124] G.J. Spencer, J.C. Utting, S.L. Etheridge, T.R. Arnett, P.G. Genever, Wnt signalling in osteoblasts regulates expression of the receptor activator of NFkappaB ligand and inhibits osteoclastogenesis in vitro, J. Cell Sci. 119 (Pt 7) (2006) 1283–1296.

[125] C. Zhang, Q. Liao, J.H. Ming, G.L. Hu, Q. Chen, S.Q. Liu, Y.M. Li, The effects of chitosan oligosaccharides on OPG and RANKL expression in a rat osteoarthritis model, Acta Cir. Bras. 32 (6) (2017) 418–428.

[126] X. Bai, D. Lu, A. Liu, Z. Zhang, X. Li, Z. Zou, W. Zeng, B. Cheng, S. Luo, Reactive oxygen species stimulates receptor activator of NF-κB ligand expression in osteoblast, J. Biol. Chem. 280 (17) (2005) 17497–17506.

[127] J.M. Lean, C.J. Jagger, B. Kirstein, K. Fuller, T.J. Chambers, Hydrogen peroxide is essential for estrogen-deficiency bone loss and osteoclast formation, Endocrinology 146 (2) (2005) 728–735.

[128] C. Wu, E.B. Rankin, L. Castellini, J. Fernandez-Alcudia, E.L. Lagory, R. Andersen, S.D. Rhodes, T.L.S. Wilson, K.S. Mohammad, A.B. Castillo, T.A. Guise, E. Schipani, A.J. Giaccia, Oxygen-sensing PHDs regulate bone homeostasis through the modulation of osteoprotegerin, Genes Dev. 29 (8) (2015) 817–831.

[129] H.J. Park, K. Baek, J.H. Baek, H.R. Kim, TNFα increases RANKL expression via PGE2-induced activation of NFATc1, Int. J. Mol. Sci. 18 (3) (2017) 1–15.

[130] R.B. Kimble, S. Bain, R. Pacifici, The functional block of TNF but not of IL-6 prevents bone loss in ovariectomized mice, J. Bone Miner. Res. 12 (6) (1997) 935–941.

[131] S. Pandiarajan, S. Samuel, T. Loganathan, S. Jaganathan, T. Krishnamurthi, R. Sarangapani, V. Anandan, R. Venkatachalam, Pila globosa snail extract inhibits osteoclast differentiation via downregulation of nuclear factor κB and nuclear factor of activated T-Cells c1 signaling pathways, Phcog. Mag. 15 (64) (2019) 298.

[132] D. Brömme, F. Lecaille, Cathepsin K inhibitors for osteoporosis and potential off-target effects, Expet Opin. Invest. Drugs 18 (5) (2009) 585–600.

[133] C. Yi, K.Y. Hao, T. Ma, Y. Lin, X.Y. Ge, Y. Zhang, Inhibition of cathepsin K promotes osseointegration of titanium implants in ovariectomised rats, Sci. Rep. 7 (2017) 1–11.

[134] H. Takatsuna, M. Asagiri, T. Kubota, K. Oka, T. Osada, C. Sugiyama, H. Saito, K. Aoki, K. Ohya, H. Takayanagi, K. Umezawa, Inhibition of RANKL-induced osteoclastogenesis by (-)-DHMEQ, a novel NF-κB inhibitor, through downregulation of NFATc1, J. Bone Miner. Res. 20 (4) (2005) 653–662.

[135] P. Valverde, Q. Tu, J. Chen, BSP and RANKL induce osteoclastogenesis and bone resorption synergistically, J. Bone Miner. Res. 20 (9) (2005) 1669–1679.

[136] A.R. Wijenayaka, M. Kogawa, H.P. Lim, L.F. Bonewald, D.M. Findlay, G.J. Atkins, Sclerostin stimulates osteocyte support of osteoclast activity by a RANKL-dependent pathway, PloS One 6 (10) (2011), e25900.

[137] G. Guo, A. Tian, X. Lan, C. Fu, Z. Yan, C. Wang, Nano hydroxyapatite induces glioma cell apoptosis by suppressing NF-κB signaling pathway, Exp. Therapeut. Med. 17 (5) (2019) 4080–4088.

[138] S. Kamolmatyakul, W. Chen, S. Yang, Y. Abe, R. Moroi, A.M. Ashique, Y.P. Li, IL-1α stimulates cathepsin K expression in osteoclasts via the tyrosine kinase-NF-κB pathway, J. Dent. Res. 83 (10) (2004) 791–796.

[139] Q. Zhao, Y. Jia, Y. Xiao, Cathepsin K: a therapeutic target for bone diseases, Biochem. Biophys. Res. Commun. 380 (4) (2009) 721–723.

[140] J. Tu, Y. Xu, J. Xu, Y. Ling, Y. Cai, Chitosan nanoparticles reduce LPS-induced inflammatory reaction via inhibition of NF-κB pathway in Caco-2 cells, Int. J. Biol. Macromol. 86 (2016) 848–856.

[141] S.I. Miller, R.K. Ernst, M.W. Bader, LPS, TLR4 and infectious disease diversity, Nat. Rev. Microbiol. 3 (1) (2005) 36–46.

[142] J. Zhu, Y. Zhang, G. Wu, Z. Xiao, H. Zhou, X. Yu, Inhibitory effects of oligochitosan on TNF-α, IL-1β and nitric oxide production in lipopolysaccharide.induced RAW264-7 cells, Mol. Med. Rep. 11 (1) (2015) 729–733.

[143] A. Cianciulli, R. Calvello, P. Cavallo, T. Dragone, V. Carofiglio, M.A. Panaro, Modulation of NF-κB activation by resveratrol in LPS treated human intestinal cells results in downregulation of PGE2 production and COX-2 expression, Toxicol. Vitro 26 (7) (2012) 1122–1128.

[144] D. Singh, M. Singh, N. Singh, Phytofabricated silver nanoparticles of phyllanthus emblica extract attenuated diethylnitrosamine induced hepatocellular carcinoma in rats via NF-κB pathway, Gut 68 (Suppl 1) (2019). A49–A49.

[145] A. Fehaid, A. Taniguchi, Size-dependent effect of silver nanoparticles on the tumor necrosis factor α-induced DNA damage response, Int. J. Mol. Sci. 20 (5) (2019) 1038.

[146] H. Liu, N. Zhang, Y. Liu, L. Liu, G. Yin, L. En, Effect of human Wnt10b Transgene overexpression on peri-implant osteogenesis in ovariectomized rats, Hum. Gene Ther. 29 (12) (2018) 1416–1427.

[147] L. Song, J. Zhao, X. Zhang, H. Li, Y. Zhou, Icariin induces osteoblast proliferation, differentiation and mineralization through estrogen receptor-mediated ERK and JNK signal activation, Eur. J. Pharmacol. 714 (1–3) (2013) 15–22.

[148] S. Mathews, P.K. Gupta, R. Bhonde, S. Totey, Chitosan enhances mineralization during osteoblast differentiation of human bone marrow-derived mesenchymal

stem cells, by upregulating the associated genes, Cell Prolif. 44 (6) (2011) 537–549.

[149] C. Liu, L. Wang, R. Zhu, H. Liu, R. Ma, B. Chen, L. Li, Y. Guo, Q. Jia, S. Shi, D. Zhao, F. Mo, B. Zhao, J. Niu, M. Fu, A.N. Orekhov, D. Brömme, S. Gao, D. Zhang, Rehmanniae Radix Preparata suppresses bone loss and increases bone strength through interfering with canonical Wnt/β-catenin signaling pathway in OVX rats, Osteoporos. Int. 30 (2) (2019) 491–505.

[150] P. Dong, D. Zhu, X. Deng, Y. Zhang, J. Ma, X. Sun, Y. Liu, Effect of hydroxyapatite nanoparticles and wedelolactone on osteoblastogenesis from bone marrow mesenchymal stem cells, J. Biomed. Mater. Res. 107 (1) (2019) 145–153.

[151] B.R. Macias, J.M. Swift, M.I. Nilsson, H.A. Hogan, S.D. Bouse, S.A. Bloomfield, Simulated resistance training, but not alendronate, increases cortical bone formation and suppresses sclerostin during disuse, J. Appl. Physiol. 112 (5) (2012) 918–925.

[152] W. Kim, Y. Chung, S.H. Kim, S. Park, J.H. Bae, G. Kim, S.J. Lee, J.E. Kim, B.W. Park, S.K. Lim, Y. Rhee, Increased sclerostin levels after further ablation of remnant estrogen by aromatase inhibitors, Endocrinol. Metab. 30 (1) (2015) 58–64.

[153] Y. Wang, F. Xue, Effect of Bushen Jiangu decoction on ovariectomyinduced osteoporosis in rats, Trop. J. Pharmaceut. Res. 18 (2) (2019) 327.

[154] C.R. Parker, P.J. Blackwell, K.J. Fairbairn, D.J. Hosking, Alendronate in the treatment of primary hyperparathyroid-related osteoporosis: a 2-year study, J. Clin. Endocrinol. Metabol. 87 (10) (2002) 4482–4489.

[155] L. Qin, W. Choy, S. Au, M. Fan, P. Leung, Alendronate increases BMD at appendicular and axial skeletons in patients with established osteoporosis, J. Orthop. Surg. Res. 2 (1) (2007) 5.

[156] M.J. Seibel, H.W. Woitge, M. Pecherstorfer, M. Karmatschek, E. Horn, H. Ludwig, F.P. Armbruster, R. Ziegler, Serum immunoreactive bone sialoprotein as a new marker of bone turnover in metabolic and malignant bone disease, J. Clin. Endocrinol. Metabol. 81 (9) (1996) 3289–3294.

[157] H. Fleisch, Bisphosphonates: pharmacology, Semin. Arthritis Rheum. 23 (4) (1994) 261–262.

[158] S. Tanaka, Molecular mechanism of the life and death of the osteoclast, Ann. N. Y. Acad. Sci. 1068 (1) (2006) 180–186.

[159] P. Rowe, S. Sharma. Physiology, Bone Remodeling.StatPearls, StatPearls Publishing, Treasure Island (FL), 2019. Bookshelf ID: NBK499863. PMID: (2019) 29763038.

[160] R.A.B. Silva, A.P. Sousa-Pereira, M.P. Lucisano, P.C. Romualdo, F.W.G. Paula-Silva, A. Consolaro, L.A.B. Silva, P. Nelson-Filho, Alendronate inhibits osteocyte apoptosis and inflammation via IL-6, inhibiting bone resorption in periapical lesions of ovariectomized rats, Int. Endod. J. (2019).

[161] D.A. Tipton, B.A. Seshul, M.K. Dabbous, Effect of bisphosphonates on human gingival fibroblast production of mediators of osteoclastogenesis: RANKL, osteoprotegerin and interleukin-6, J. Periodontal. Res. 46 (1) (2011) 39–47.

[162] W. Yang, H. Ko, H. Kim, M. Kim, The effect of cathepsin K inhibitor on osteoclastic activity compared to alendronate and enamel matrix protein, Dent. Traumatol. 31 (3) (2015) 202–208.

[163] K. Diercke, A. Kohl, C.J. Lux, R. Erber, IL-1β und Kompression führen zu einer signifikanten Induktion der RANKL-Expression in primären humanen Zementoblasten, J. Orofac. Orthop. 73 (5) (2012) 397–412.

[164] M. Muñoz-Torres, R. Reyes-García, P. Mezquita-Raya, D. Fernández-García, G. Alonso, J.d. Dios Luna, M.E. Ruiz-Requena, F. Escobar-Jiménez, Serum cathepsin K as a marker of bone metabolism in postmenopausal women treated with alendronate, Maturitas 64 (3) (2009) 188–192.

[165] J. Yu, N.S. Adapala, L. Doherty, A. Sanjay, Cbl-PI3K interaction regulates Cathepsin K secretion in osteoclasts, Bone 127 (2019) 376–385.

[166] R. Inoue, N.A. Matsuki, G. Jing, T. Kanematsu, K. Abe, M. Hirata, The inhibitory effect of alendronate, a nitrogen-containing bisphosphonate on the PI3K-Akt-NFκB pathway in osteosarcoma cells, Br. J. Pharmacol. 146 (5) (2005) 633–641.

[167] Y. Imai, T. Hasegawa, D. Takeda, M. Akashi, T. Komori, The osteogenic activity of human mandibular fracture haematoma-derived progenitor cells is affected by bisphosphonate in vitro, Int. J. Oral Maxillofac. Surg. 44 (3) (2015) 412–416.